

AL/OE-TR-1994-0048

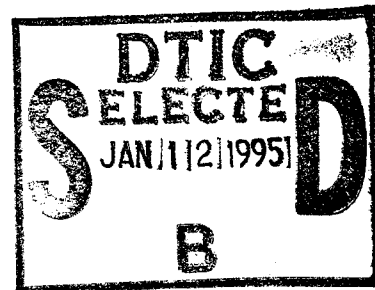


THE USE OF STRUCTURAL-ACOUSTIC RECIPROcity  
TECHNIQUES TO ASSESS POTENTIAL ENVIRONMENTAL  
(STRUCTURAL) DAMAGE FROM SONIC BOOMS

Joel Garrelick  
Kyle Martini

CAMBRIDGE ACOUSTICAL ASSOCIATES, INC.  
200 BOSTON AVENUE, SUITE 2500  
MEDFORD, MASSACHUSETTS 02155-4243

19950111 091



DECEMBER 1993

DTIC QUALITY INSPECTED 3

FINAL REPORT FOR THE PERIOD MAY 1993 TO DECEMBER 1993

Approved for public release; distribution is unlimited

AIR FORCE MATERIEL COMMAND  
WRIGHT-PATTERSON AIR FORCE BASE, OHIO 45433-6573

ARMSTRONG  
LABORATORY

## NOTICES

When US Government drawings, specifications, or other data are used for any purpose other than a definitely related Government procurement operation, the Government thereby incurs no responsibility nor any obligation whatsoever, and the fact that the Government may have formulated, furnished, or in any way supplied the said drawings, specifications, or other data, is not to be regarded by implication or otherwise, as in any manner licensing the holder or any other person or corporation, or conveying any rights or permission to manufacture, use, or sell any patented invention that may in any way be related thereto.

Please do not request copies of this report from the Armstrong Laboratory. Additional copies may be purchased from:

National Technical Information Service  
5285 Port Royal Road  
Springfield, Virginia 22161

Federal Government agencies registered with the Defense Technical Information Center should direct requests for copies of this report to:

Defense Technical Information Center  
Cameron Station  
Alexandria, Virginia 22314

### DISCLAIMER

This Technical Report is published as received and has not been edited by the Technical Editing Staff of the Armstrong Laboratory.

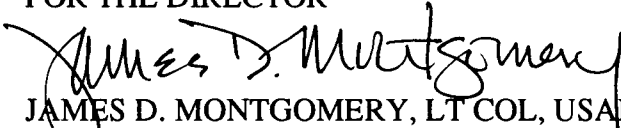
### TECHNICAL REVIEW AND APPROVAL

AL/OE-TR-1994 -0048

This report has been reviewed by the Office of Public Affairs (PA) and is releasable to the National Technical Information Service (NTIS). At NTIS, it will be available to the general public, including foreign nations.

This technical report has been reviewed and is approved for publication.

FOR THE DIRECTOR

  
JAMES D. MONTGOMERY, LT COL, USAF, BSC  
Chief

Bioenvironmental Engineering Division  
Armstrong Laboratory

# REPORT DOCUMENTATION PAGE

Form Approved  
OMB No. 0704-0188

Public reporting burden for this collection of information is estimated to average 1 hour per response, including the time for reviewing instructions, searching existing data sources, gathering and maintaining the data needed, and completing and reviewing the collection of information. Send comments regarding this burden estimate or any other aspect of this collection of information, including suggestions for reducing this burden, to Washington Headquarters Services, Directorate for Information Operations and Reports, 1215 Jefferson Davis Highway, Suite 1204, Arlington, VA 22202-4302, and to the Office of Management and Budget, Paperwork Reduction Project (0704-0188), Washington, DC 20503.

<b>1. AGENCY USE ONLY (Leave blank)</b>		<b>2. REPORT DATE</b> December 1993	<b>3. REPORT TYPE AND DATES COVERED</b> Final - 17 May 93 thru 17 Dec 93	
<b>4. TITLE AND SUBTITLE</b> The Use of Structural-Acoustic Reciprocity Techniques To Assess Potential Environmental (Structural) Damage From Sonic Booms			<b>5. FUNDING NUMBERS</b> C - F41624-93-C-9004 PE - 62202F PR - 3005 TA - OB WU - 3A	
<b>6. AUTHOR(S)</b> Joel Garrelick Kyle Martini				
<b>7. PERFORMING ORGANIZATION NAME(S) AND ADDRESS(ES)</b> Cambridge Acoustical Associates, Inc. 200 Boston Avenue, Suite 2500 Medford, Ma 02155-4243			<b>8. PERFORMING ORGANIZATION REPORT NUMBER</b>	
<b>9. SPONSORING/MONITORING AGENCY NAME(S) AND ADDRESS(ES)</b> Armstrong Laboratory, Noise Effects Branch Bioenvironmental Engineering Division Human Systems Center Air Force Materiel Command Wright-Patterson AFB OH 45433-7901			<b>10. SPONSORING/MONITORING AGENCY REPORT NUMBER</b>  AL/OE-TR-1994-0048	
<b>11. SUPPLEMENTARY NOTES</b>				
<b>12a. DISTRIBUTION / AVAILABILITY STATEMENT</b>  Approved for public release; distribution is unlimited			<b>12b. DISTRIBUTION CODE</b>	
<b>13. ABSTRACT (Maximum 200 words)</b> The potential environmental impact of supersonic operations includes damage to conventional and unconventional structures by sonic boom overpressures. The assessment of such damage requires dedicated flyovers for each site at great expense. We show that structural-acoustic techniques may be used to help provide such assessments in their absence. Tests are described whereby transfer functions relating structural response to sonic boom overpressure may be obtained using a stationary acoustic source and appropriate data processing to substitute for the boom. Further, structural-acoustic reciprocity is invoked allowing these transfer functions to be determined by measuring the sound radiated by the structure when driven mechanically. Additionally, it is demonstrated that state-of-the-art general purpose computer codes now provide a powerful tool for predicting these transfer functions for complex site geometries and constructions.				
<b>14. SUBJECT TERMS</b> sonic boom damage assessment structural acoustics			<b>15. NUMBER OF PAGES</b> 54	
			<b>16. PRICE CODE</b>	
<b>17. SECURITY CLASSIFICATION OF REPORT</b> UNCLASSIFIED	<b>18. SECURITY CLASSIFICATION OF THIS PAGE</b> UNCLASSIFIED	<b>19. SECURITY CLASSIFICATION OF ABSTRACT</b> UNCLASSIFIED	<b>20. LIMITATION OF ABSTRACT</b> UNLIMITED	

THIS PAGE LEFT BLANK INTENTIONALLY

TABLE OF CONTENTS

	Page
1. SUMMARY . . . . .	iv
2. INTRODUCTION . . . . .	1
2.1 STRUCTURAL DAMAGE ASSESSMENT . . . . .	1
2.2 STRUCTURAL-ACOUSTIC RECIPROCITY . . . . .	8
2.2.1 Background . . . . .	8
2.2.2 Proposed Application . . . . .	9
3. STRUCTURAL-ACOUSTIC PREDICTIVE MODELS FOR THE RESPONSE OF STRUCTURES TO SONIC BOOMS . . . . .	14
3.1 THE ILLUMINATED AIRBORNE PATH . . . . .	14
3.1.1 Plate Response To Incident Acoustic Wave . . . . .	16
3.1.2 Sound Radiated By Mechanically Driven Plate . . . . .	19
3.1.3 Numerical Results . . . . .	20
3.2 THE DIFFRACTED AIRBORNE PATH . . . . .	24
3.2.1 The Helmholtz Integral Equation . . . . .	30
3.2.2 Illustrative Example . . . . .	32
3.2.3 Numerical Results . . . . .	35
3.3 THE SEISMIC PATH . . . . .	37
4. CONCLUSIONS AND RECOMMENDATIONS . . . . .	46
5. REFERENCES . . . . .	48

<b>Accession For</b>	
NTIS GRA&I	<input checked="" type="checkbox"/>
DTIC TAB	<input type="checkbox"/>
Unannounced	<input type="checkbox"/>
Justification	
By _____	
Distribution/_____	
<b>Availability Codes</b>	
Dist	Avail and/or Special
A-1	

## SUMMARY

The potential environmental impact of supersonic operations includes damage to conventional and unconventional structures by sonic boom overpressures. The assessment of such damage generally requires dedicated flyovers for each site at great expense. In this report we show that structural-acoustic techniques may be used to help provide such assessments in their absence. These techniques allow for both airborne and groundborne propagation paths and also account for diffraction. Tests are described whereby transfer functions relating structural response to sonic boom overpressure may be obtained using a broad band stationary acoustic source and appropriate data processing to substitute for the boom. Further, structural-acoustic reciprocity is invoked allowing these transfer functions to be determined by measuring the sound radiated by the structure when driven mechanically. Additionally, it is demonstrated that state-of-the-art general purpose finite element-boundary element structural-acoustic computer codes, which inherently satisfy reciprocity, now provide a powerful analytical tool for predicting these transfer functions for complex site geometries and constructions. Finally, it is suggested that (1) empirical validation of the above techniques be pursued by comparison with data taken at a series of sites/structures with actual supersonic flyovers, and (2) upon successful completion of (1), the necessary procedures be codified to provide a new structural damage assessment tool for those responsible for site planning and development and operations planning in vulnerable environments.

## INTRODUCTION

The potential environmental impact of the U.S. Air Force or commercial supersonic operations extends to humans and other animals and structures, both conventional and unconventional. Damage may be psychological or physiological in the first case and cosmetic or structural in the second. The source of such damage is the pressure field of the sonic "boom". Performing an environmental damage assessment typically requires dedicated aircraft flyovers for each site, at great expense. This study investigates a technique for providing such assessments in their absence, and focuses on damage to structures. The approach uses structural-acoustic tests in the reciprocal mode. It is based on the assumption that the boom pressure levels are in the linear range in the immediate vicinity of the subject structures. With this approach a stationary vibration source, an array of microphones and digital post processing of the measured signals substitute for actual flyovers. In Section 2.1 below we briefly review current procedures for relating damage assessment to measurements. A brief background of structural-acoustic reciprocity is provided in Section 2.2.1 and in 2.2.2 we outline the general procedure for the proposed application.

### 2.1 STRUCTURAL DAMAGE ASSESSMENT

Sonic boom induced damage to structures is generally envisioned in terms of a maximum stress. That is damage occurs if and when a supersonic operation causes a stress somewhere in the structure to exceed a material strength. For example, plaster walls and windows are particularly susceptible.<sup>1</sup> However stress is not a readily measured quantity. As a consequence surrogate measures coupled with some level of analytical modelling is required. For example the theory of linear elasticity allows one to compute stress from strain measurements using rosette strain gages and estimates of material elastic moduli. Peak stresses may also be

predicted from measurements of structural surface pressures or motions by cascading transfer functions, analytically or empirically determined. For example,<sup>2</sup>

$$\sigma_{pk} = P_a(\sigma_{pk}/P_a) = P_{ff}(P_a/P_{ff})(\sigma_s/P_a)DAF \quad (1)$$

with the dynamic amplification factor

$$DAF = \sigma_{pk}/\sigma_s \quad (2)$$

where

$\sigma_{pk}$  = peak dynamic stress at a given location  $\bar{x}$  on the structure in response to  $P_a$

$\sigma_s$  = stress at  $\bar{x}$  in response to statically applied pressure with magnitude  $P_a$ .

$P_{ff}$  = free field acoustic pressure

$P_a$  = pressure on the structure

The first ratio in Eq. 1 accounts for the effects of acoustic diffraction around, and reflections from, nearby obstacles including the structure in question. In the absence of such effects the ratio is unity. The second ratio characterizes the induced stress in the structure by the boom pressure, ignoring dynamic effects which are accounted for separately in the DAF.

In Eq. 1 it is generally the case that the quantities  $P_{ff}$  and perhaps  $(P_a/P_{ff})$  are measured during a flyover while the other functions are estimated analytically.

An alternative formulation<sup>2</sup> defines

$$(\sigma_{pk}/P_a) = (\sigma_{pk}/V_{pk})(V_{pk}/P_a) \quad (3)$$

and therefore

$$\sigma_{pk} = P_a(\sigma_{pk}/V_{pk})(V_{pk}/P_a) \quad (4)$$



where

$V_{pk}$  = peak structural velocity at  $\bar{x}$  in response to the applied pressure. The advantage of Eq. 4 is that, under a reasonably broad range of circumstances the ratio  $(\sigma_{pk}/V_{pk})$  may be determined from impedance-like structural measurements.<sup>3,4</sup> Therefore  $\sigma_{pk}$  becomes a function of a directly measurable quantity, possibly but not necessarily, during a flyover. For example, it may be shown that this ratio takes on the simple form

$$\sigma_{pk}/V_{pk} = K\rho_p c_p \quad (5)$$

where  $\rho_p$  is the surface mass density and  $c_p$  the compressional sound speed in the material with  $K=1$  for compressional waves in a rod,  $K=\sqrt{3}$  for a rectangular beam in flexure and  $1.12 < K < 2.0$  for flexing plates with aspect ratios ranging broadly from 0.1 to 1.0.

To this point the applicable damage assessment metric has been taken to be peak stress, either directly or indirectly via peak velocity. However in some cases stress is not necessarily the most useful measure. As an example consider the rattling of bric-a-brac articles, and in particular the onset of rattling which may provide a more practical criterion than actual breakage.

Assume that the rattling of bric-a-brac articles follows immediately the onset of their sliding relative to some sonic boom induced base motion. Then, assuming a horizontal base acceleration,  $a_b$ , and a one dimensional translational model, slippage is avoided provided that  $a_b < \mu g$ , where  $\mu$  is an appropriate coefficient of static friction and  $g$  the acceleration of gravity. Typically  $\mu < 1$ , for example 0.4-0.7 for stone on stone and 0.25-0.5 for wood on wood. Therefore this yields a more stringent criterion than had we considered a vertical base motion and rattling associated with loss of contact, for which the criterion is  $a_b < g$ . To account for tipping one must

introduce the center of gravity and the moment of inertia of the article. However, here too the criterion may be expressed in terms of the base acceleration.

For perspective, a sampling of empirically based damage criteria for the peak stress and structural velocity of conventional and unconventional structures is shown in Tables 1 and 2 along with a qualitative ranking of damage susceptibility by structure type for historical structures in Table 3.<sup>5</sup> Interestingly, the levels shown in Tables 1 and 2 are by and large lower than those given in Ref. 6 for "particle velocities that are the threshold of possible damage for both commercial structures and residential-type structures", viz., 4 and 1 in/sec respectively.

The distinction between conventional and unconventional, or historical, or as suggested in Ref. 2 irreplaceable, structures is not fundamental to the validity of structural-acoustic testing. Rather the issues relate to practicality, for example testing accessibility, and the precision of the damage assessment, for example owing to uncertainties in material properties associated with aging. The latter is likely in evidence in the spread of data shown in Tables 1 and 2.

In theory structural-acoustic reciprocity is compatible with all of the above approaches to damage assessment. In practice, however, the reciprocal testing of complex states of stress/strain is not deemed feasible and we will confine ourselves to the measurement of the other metrics, viz., surface pressures and structural accelerations, velocities and displacements, to be used in conjunction with appropriate transfer functions.

Table 1. Estimated Failure Stress Values for Glass Panes and Masonry Walls (Tables 4-4 and 4-6 of Ref. 2).

Comparison of Failure Load and Estimated Failure Stress of Old vs. New Glass Window Panes of Thickness h and Side Dimensions a, b (Data from Beason and Morgan, 1984)

Sample	Age, Years	Sample Size	h, in.	a, in.	b, in.	P, Failure Load (Mean ± S.D.)		Estimated Failure Stress	
						psf	psi	Linear <sup>(4)</sup>	Nonlinear <sup>(5)</sup>
GPL (1)	20	20	2.128	28.5	60.5	79 ± 23.3%	6,100	1,790	
GPL (1)	20	20	2.128	28.5	60.5	168 ± 22.3%	6,105	3,370	
Dallas (2)	20	22	.125	16.25	19.75	229 ± 27%	10,480	4,210	
Anton (3)	25	132	.25	14	36.25	134.3 ± 25.1%	1,272	522	
							Log Mean (all samples)	5,245	1,970
							Log Mean (without Anton samples)	7,270	2,940
New	0	NA	.125	16.25	19.75	427.7 ± 18.1%	19,575	6,205	

$$\text{Average ratio of failure stress} = \left\{ \frac{\text{(linear model)}}{\text{(nonlinear model)}} \right\} = \left\{ \frac{3.15, \text{ new glass}}{2.66, \text{ old glass}} \right\}$$

Notes:

- (1) Samples from GPL Building, Lubbock Texas (from Building Renovation)
- (2) Samples from Johnson Chevrolet Building, Dallas Texas (from Building Renovation)
- (3) Samples from Public School Building, Anton Texas (from Building Salvage)
- (4) Stress,  $\sigma$  (failure) =  $K \cdot (a/h)^2$ , where  $K$  = function (a/b), linear model (Roark, 1965)

Note that this relationship between the factor  $K$  and the panel aspect ratio for this linear stress prediction equation is more complex than has been assumed by others (Hershey and Higgins, 1976; Faber and Nakaki, 1989) and correctly predicts stresses which are 15% to 50% higher for a simply supported plate with aspect ratios of 1:1 and less than 0.2 respectively than the incorrect equation utilized in these prior studies.

- (5) Stress,  $\sigma$  (failure) computed from non-linear theory (from Seaman, 1967)
 
$$Q = 4.93 S_b + 0.0329 S_b^3$$
 where  $Q = P(a/h)^2/E$ , nondimensional load  
 $S_b = \sigma(a/h)^2/E$ , nondimensional bending stress  
 $P$  = Static Pressure Load  
 $E$  = Young's Modulus

Summary of Estimated Failure or Damage Stress Values for Various Types of Masonry Walls Based on (a) Blast Damage Criteria and (b) Static Test Data

Type of Masonry Wall	Thickness in.	Level of Damage <sup>(5)</sup>	Peak Velocity in/sec	E/CL psi/in/s	Estimated Stress <sup>(4)</sup> psi
<b>(a) Blast Damage Criteria</b>					
Stone and Mortar Basement Walls (1)	18-24	None	3.4 ± 1.3	48.2 ± 12.5	220 ± 110
	18-24	Minor	10.3		665 ± 175
Stone and Mortar (1)	NA	None	3.4		220 ± 58
	NA	Threshold	4.5		284 ± 75
	NA	Minor	7.0		452 ± 118
	NA	Major	10.0		646 ± 168
Concrete Block (1)	8-10	None	3.0	13.1 ± 6.5	53 ± 27
	8-10	Threshold	3.0+		53 ± 27
	7-9	Threshold	10.0		176 ± 87
Brick Wall (1)	4	Threshold	>12 (6)	17.2 ± 4.8	>280 ± 77(6)
<b>(b) Static Test Data</b>					
Brick Wall (2)	4	First Cracks	NA	0.418 ± 153%	
Brick Wall (3)	6-8	NA	NA	0.528 ± 410%	
	4-8		Average	0.473	55 (7)
Brick Wall 1:3 mortar <sup>(8)</sup>	4-8	Failure	NA	NA	18.5 ± 10.3(8)
Brick Wall, high bond mortar <sup>(8)</sup>	4-8	Failure	NA	NA	190 ± 84 (8)

- (1) Stagg, et al., 1984
- (2) Hershey and Higgins, 1976, average for two samples of four different walls with low strength (1:1:4 mix) and high bond mortar.
- (3) Average for four mortar mixes, low to high strength (Appendix B).
- (4) Estimated damage stress, in psi,  $\sigma = K_S \cdot (E/CL) = 48.2 \text{ psi}/(\text{in}/\text{sec})$  for typical masonry walls (see Table 4-1 and text in Section 4.2.1).
- (5) Level of damage as defined in Uniform Classification Scheme (Siskind, et al., 1980b)
- (6) Estimated based on Peak Strain > 160  $\mu$  in/in (Stagg, et al., 1984),  $E = 1.72 \times 10^6$  psi and  $K_S = 1.34$ .
- (7) Estimated based on  $\sigma = K \cdot (a/h)^2$  ps and  $K(a/h)^2 = 116$  for 4 ft x 8 ft brick wall test specimen.
- (8) Yokel, et al., 1971, estimated stress is actually computed modulus of rupture assuming partial end fixity.

Table 2. Criteria for Maximum Structural Displacement and Velocities to Avoid Damage to Prehistoric, Historic, Sensitive and Conventional Structures (Table 4-7 of Ref. 2).

Reference	Type of Structure	Frequency Range Hz	Displacement inches	Criteria Velocity in/sec
King and Algemissen, 1987	Prehistoric (Chaco Canyon)	1-20		0.08 (1)
King, et al., 1985	Prehistoric (Hovenweep)	1-10		0.004 (2)
Saurenman, et al., 1982	Historic/Sensitive			0.04 (1)
Konon and Schuring, 1985	Historic/Sensitive	< 10 Hz > 40 Hz		0.25 (1) 0.5 (1)
German DIN 4150 (3)	Ancient ruins and historic buildings Buildings with visible damage/cracks in masonry Buildings in good condition with possible cracks in plaster Industrial and concrete structures without plaster			0.08 (2) 0.16 (2) 0.32 (2) 0.4-1.56 (2)
Australian Standard (3)		<15 >15	0.008	0.75 (2) 0.75 (2)
U.K (3)	(Blasting only) (Steady state vibration)			0.4-1 (2) 0.2 (2)
Ashley (3)	Ancient and historic monuments Housing in poor repair Good residential, commercial and industrial structures Welded gas mains, sewers, engineered structures			0.3 (2) 0.47 (2) 1.0 (2) 2.0 (2)
Esteves (3)	Historical monuments, hospitals, very tall buildings Current construction Reinforced construction (e.g., earthquake resistant)			0.1-0.4 (4) 0.2-0.8 (4) 0.6-2.4 (4)
Siskind, et al., 1980a (See Figure 4-5)	Wood frame (plaster interior)	<2.7 2.7-10 10-40 >40	0.03 0.008	0.50 2.0

- (1) Peak velocity of structure
- (2) Peak velocity of ground at base of structure
- (3) As cited in Siskind, et al., 1980b, Appendix A
- (4) Range of velocities for ground varying from incoherent loose soil (lowest velocity) to coherent hard soil or rock

Table 3. Ranking\* of Historical Structures According to Susceptibility to Damage from Aircraft Noise (Table 4.1 of Ref. 5).

Type of Structure	Sonic Boom	Subsonic Jet	Heavy Helicopter
<b>Historic Sites</b>			
Windows	6	2	2
Wood frame, plaster	3	3	1
Wood frame, wood panels	8	7	7
Adobe	7	10	8
Masonry, stone	13	13	13
Brick	2	9	10
<b>Prehistoric Sites</b>			
Masonry/Stone - roof intact	4	1	3
Adobe - roof intact	5	4	5
Masonry/stone - no roof	11	5	6
Adobe - no roof	10	8	9
<b>Seismically-sensitive Areas</b>			
Avalanche - loose snow	1	6	4
Early American pictographs, petroglyphs, caves	12	11	11
Avalanches - slab	9	12	12
Landslide areas	14	14	14

\*Rank order 1 is most susceptible, 14 is least susceptible.

## 2.2 STRUCTURAL-ACOUSTIC RECIPROCITY

### 2.2.1 Background

The concept of reciprocity for linear structural-acoustic systems dates back to the mid-nineteenth century. Helmholtz's Reciprocity Principle (1860) states that an acoustic signal remains invariant when the locations of a compact source and receiver are interchanged in a homogeneous acoustic medium containing rigid boundaries. This result was generalized by Rayleigh<sup>7</sup> to include more realistic situations, for example, non-compact, i.e., extended sources and receivers, the presence of elastic scattering boundaries and dissimilar, coupled acoustic media. He also was able to show that steady flow could be accommodated provided its direction is reversed in the reciprocal situation, a result further explored by Lyamshev.<sup>8,9</sup> On the other hand it has been shown that reciprocity is violated by systems encompassing gyroscopic forces and certain classes of dissipative constraints,<sup>8</sup> factors not believed to be crucial to the proposed application.

The statement of reciprocity in the field of mechanics is known as Betti's theorem. Lyamshev and others have shown that reciprocity remains valid for steady-state structural-acoustic or elasto-acoustic systems where the structure is driven either mechanically or acoustically.<sup>9,10</sup> The dynamics of these systems may involve all forms of wave motion, e.g., compression, shear, flexure, torsion etc. Chertock showed that reciprocity was satisfied for the nonsteady or transient problem as well, while investigating the response of a submerged complex structure to an underwater explosion.<sup>11</sup>

Structural-acoustic reciprocity has been applied, extensively and successfully, to a wide range of practical problems. These include the study of structures submerged underwater where the coupling between the structure and the acoustic medium is strong,

and structures vibrating in air where the coupling is generally weak. The calibration of microphones and hydrophones is perhaps the earliest application.<sup>12</sup> Another utilization is the evaluation of the structure-borne noise component of propeller induced aircraft cabin noise.<sup>13</sup> Of particular note is the work of Ten Wolde, et al who have achieved considerable success with their reciprocity experiments aimed at diagnosing parallel structural propagation paths from vibrating ship-board equipment to sound radiation in the water.<sup>14</sup>

### 2.2.2 Proposed Application

Our generic problem is pictured in Fig. 1. An aircraft travelling supersonically produces a sonic "boom", which at some distance from the source propagates linearly as an acoustic pulse. The pressure field impinges on the ground and other obstacles, i.e., structures, at an angle  $\alpha = \sin^{-1}(1/M)$  with  $M = U/c$  where  $U$  is the flight speed,  $c$  the in air sound speed and  $M$  the effective Mach number. In the vicinity of a structure the pressure field is partially diffracted and reflected. In addition it may transmit energy into any structure either directly or indirectly after propagating along the ground, generally in the form of Rayleigh surface waves. All such effects may produce stress on the structure and therefore potentially cause damage. And all these effects are accounted for with our reciprocal approach which we now describe.

We refer to the geometry of Fig. 2a as the "direct" problem and for convenience it will be analyzed in the frequency rather than time domain. Specifically, we assume that a distant harmonic acoustic source, of volume velocity  $\dot{Q}(\bar{R};\omega)$  is responsible for the pressure field incident on the structure. Although the pressure field near the source may be highly nonlinear we take the field in the vicinity of the structure to be linear. This source is our far field representation of the sonic boom

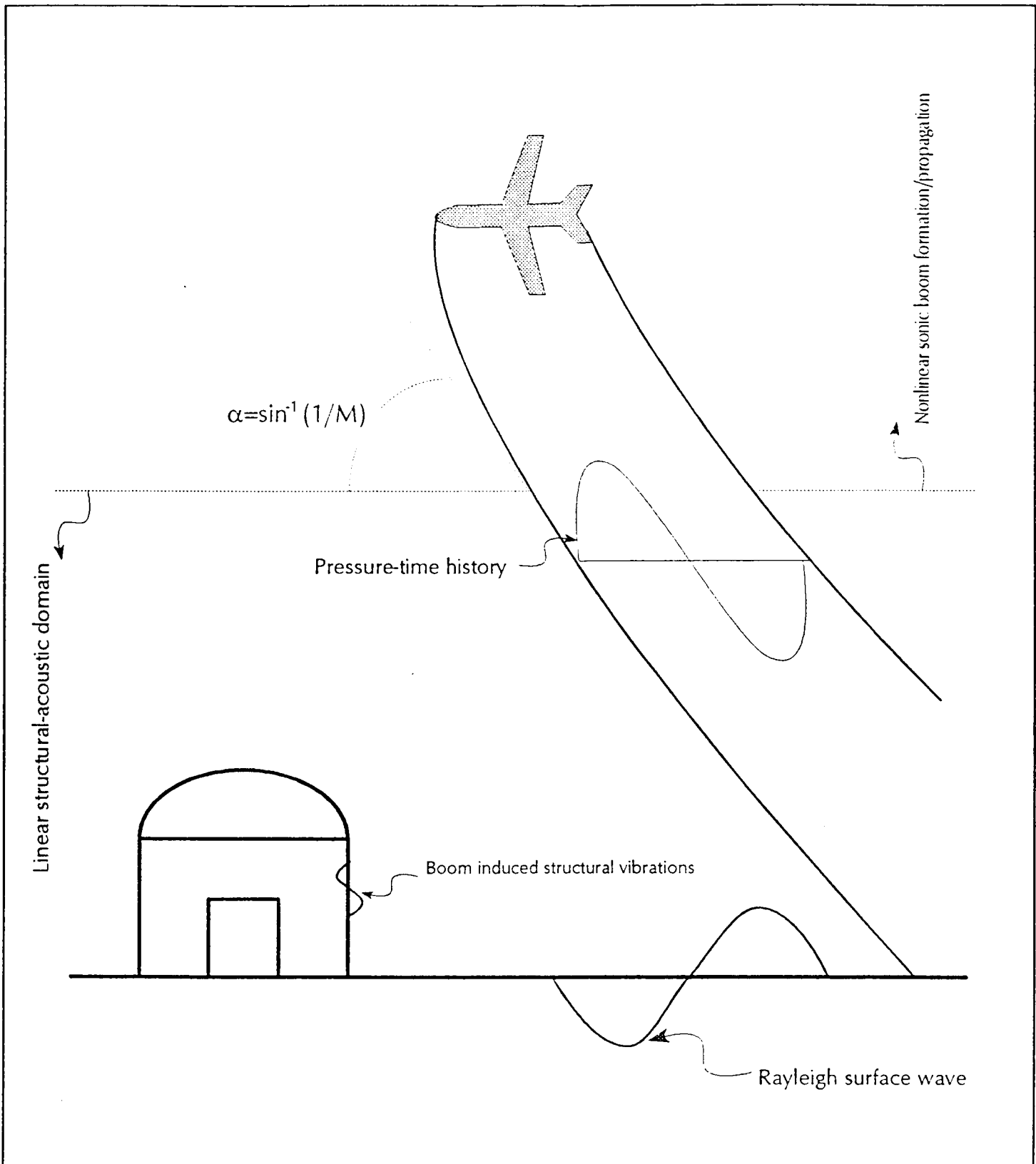


Fig 1. Sketch of Sonic Boom-Structure Geometry



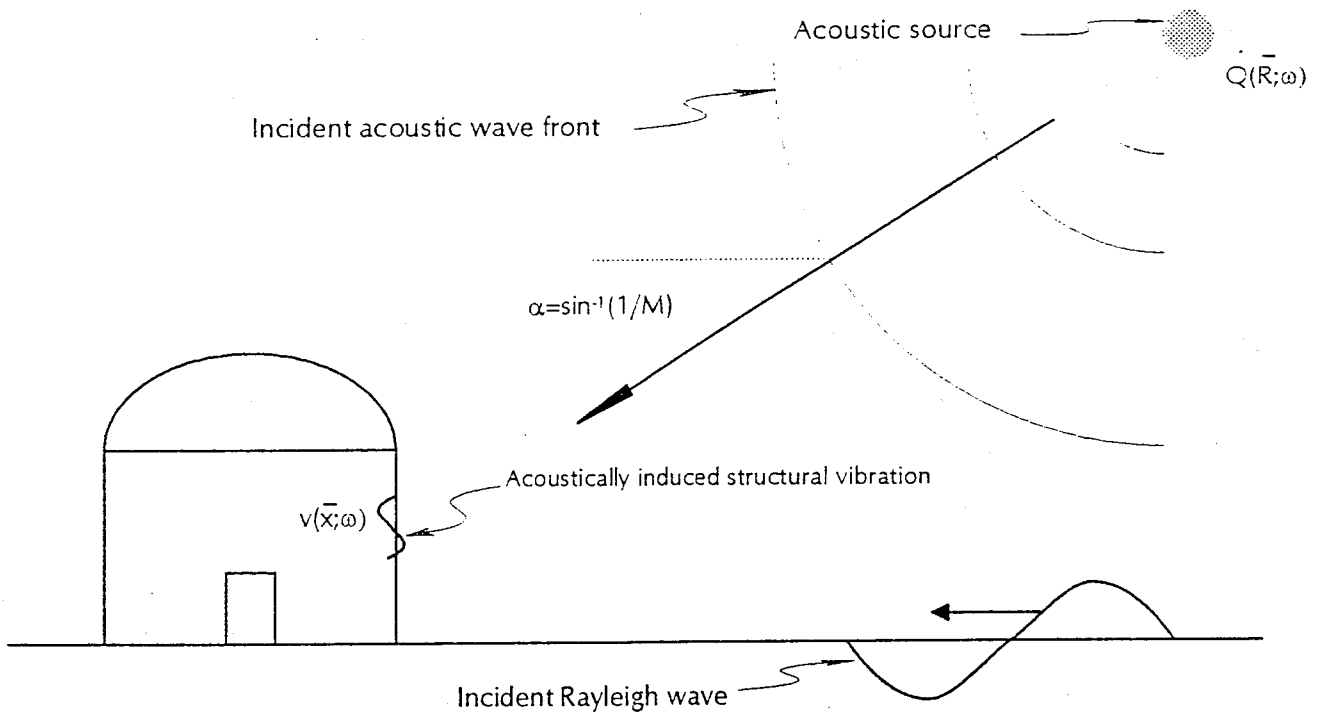


Fig 2a. Direct Structural-Acoustic Geometry

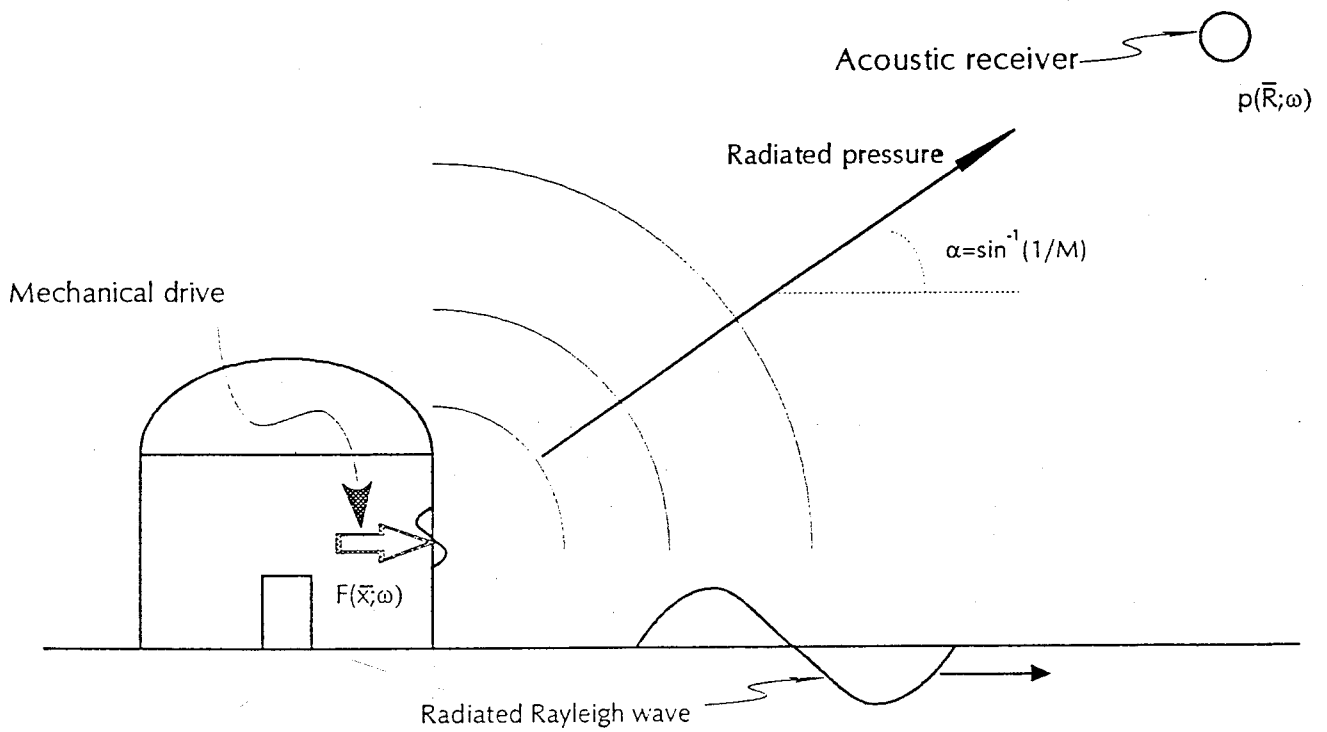


Fig 2b. Reciprocal Structural-Acoustic Geometry

generation. It is defined as the equivalent acoustic source that reproduces the incident pressure field on the structure for a given flyover,  $p_{ff}(\bar{R}';\omega)$ . Assuming a simple monopole source

$$\dot{Q}(\bar{R};\omega) = [4\pi |\bar{R}' - \bar{R}| / (-i\omega\rho)] \exp[-ik |\bar{R}' - \bar{R}|] p_{ff}(\bar{R}';\omega) \quad (6)$$

where  $\rho$  is the air density, and  $k = \omega/c$  the acoustic wavenumber at frequency  $\omega$ . The structure responds linearly, but otherwise generally as an elastic or viscoelastic fabrication, with velocity  $v(\bar{x};\omega)$ .

We now pose the "reciprocal" situation sketched in Fig. 2b. A harmonic force  $F(\bar{x};\omega)$  is applied to our structure at  $\bar{x}$ . The structure vibrates in response, producing the acoustic field  $p(\bar{R};\omega)$ . Invoking reciprocity<sup>14</sup>

$$\frac{v(\bar{x};\omega)}{\dot{Q}(\bar{R};\omega)} = \frac{p(\bar{R};\omega)}{F(\bar{x};\omega)} \quad (7)$$

or

$$v(\bar{x};\omega) = \dot{Q}(\bar{R};\omega) p(\bar{R};\omega) / F(\bar{x};\omega) \quad (8)$$

If we now interpret  $\dot{Q}(\bar{R};\omega)$  as the frequency spectrum of a time signature then the time series of the response becomes

$$v(\bar{x};t) = (2\pi)^{-1} \int_{-\infty}^{\infty} v(\bar{x};\omega) e^{-i\omega t} d\omega \quad (9)$$

and the peak velocity may be determined. In other words, the peak velocity of our structure at any and all locations in response to an incident pressure field may be determined by mechanically driving the structure at that location and measuring the associated radiated pressure. Wind or other anomalous propagation factors are of little consequence since range requirements are at most the order of acoustic wavelengths.

The only requirement on the spectrum of the mechanical source is adequate signal to noise over the frequency band of interest. It need not mimic the spectrum of the boom since the reciprocal relationship being invoked in Eq. 7 is in the form of a spectral ratio. For example any particular boom spectrum may be synthesized by post processing impulse data using an instrumented hammer. We now show that the force levels required for reciprocal testing are moderate.

The pressure radiated to range  $R$  by a point driven, effectively infinite, thin elastic panel may be estimated from

$$|P_{rad}(R;\omega)| = (\rho/\rho_p)F/2\pi R h$$

where  $F$  is the spectral level of the force,  $(\rho/\rho_p)$  the ratio of air to panel mass densities and  $h$  is the panel thickness. For illustrative purposes, taking a 1 lb. (4.4N) force on a 2.5 cm thick wood panel of specific gravity 0.5 at a nominal range of 1m, we obtain the (frequency invariant) pressure spectral level of roughly 70 dB re 0.0002  $\mu$ bar. The corresponding drive acceleration of this panel is given by

$$|a(\omega)| = (\sqrt{3}/4)\omega F/\rho_p c_p h^2$$

where  $c_p$  is the sound speed in the panel material. Letting  $c_p = 3.5 \times 10^3$  m/sec, this force yields a drive acceleration of  $-60 + 20 \log f$  (Hz) dB re 1g. For perspective, the acceleration of our effectively infinite panel to a normally incident acoustic wave of magnitude  $p_i$  is given by the mass law,

$$|a| = 2p_i/\rho_p h$$

and for instance a 1 psf (47.3 N/m<sup>2</sup>) incident pressure yields an acceleration level of -2.5 dB re 1g.

### 3. STRUCTURAL-ACOUSTIC PREDICTIVE MODELS FOR THE RESPONSE OF STRUCTURES TO SONIC BOOMS

The excitation of a structure by the pressure field of a sonic boom may be both airborne and seismic and may result from direct and/or diffracted pressure components. In the following three subsections we demonstrate structural-acoustic reciprocity for each of these phenomena, treated separately for the sake of simplicity. Both analytical models (Sections 3.1 and 3.3) and a numerical model (Section 3.2) are presented to display the broad spectrum of predictive tools that are now available, particularly with general purpose structural-acoustic finite element-boundary element (FE/BE) computer codes.

#### 3.1 THE ILLUMINATED AIRBORNE PATH

To analyze the airborne path for illuminated structural elements we consider the idealized geometry shown in Fig. 3.a. A plane wave is incident on a simply supported rectangular thin plate. The plate, which may be orthotropic to simulate the effects of framing, responds in flexure. Vibrational energy dissipation is accounted for by means of a structural loss factor ( $\eta$ ) which is incorporated into the elastic modulus ( $E$ ), making it complex, i.e.,  $E \Rightarrow E(1 - i\eta)$ . In computing the drive pressure on the plate it is assumed to be baffled. The approach is to first obtain the solution in the frequency domain for a pure impulse. The solution for a given waveform, or pressure time history, is then obtained by performing the necessary convolution, or inverse (Fourier) transform. Next, it is shown that this solution may be interpreted reciprocally as the sound pressure radiated by the plate when driven mechanically. Finally, numerical results are presented for an illustrative example and related to peak stress.

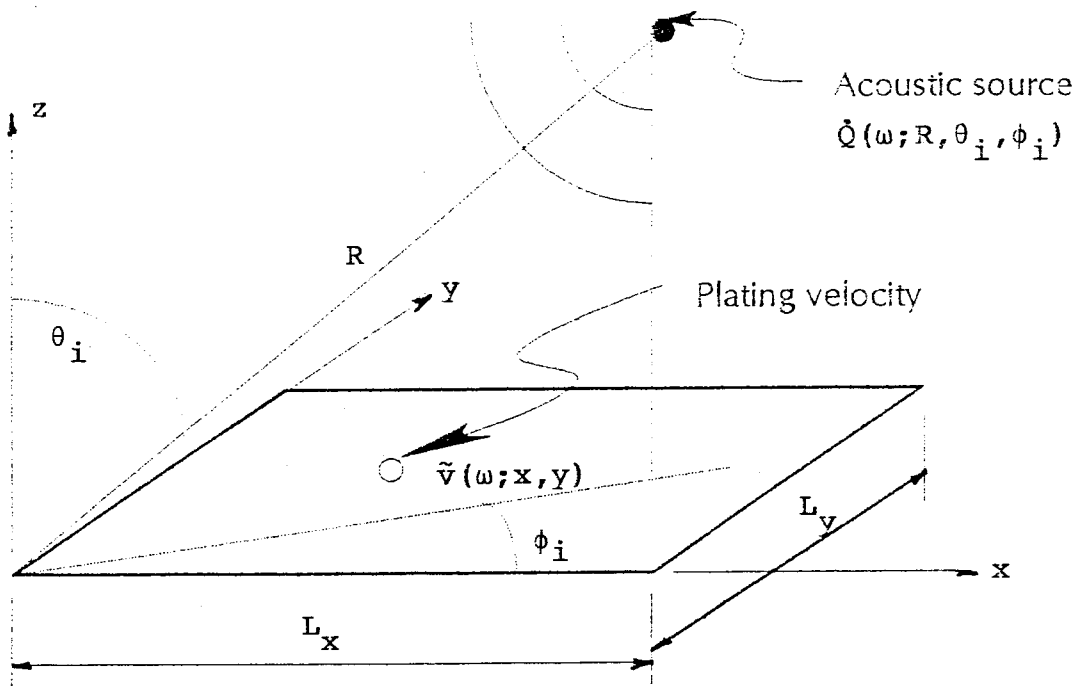


Fig 3a. Simply Supported Plate Insonified By Acoustic Source: Direct Geometry

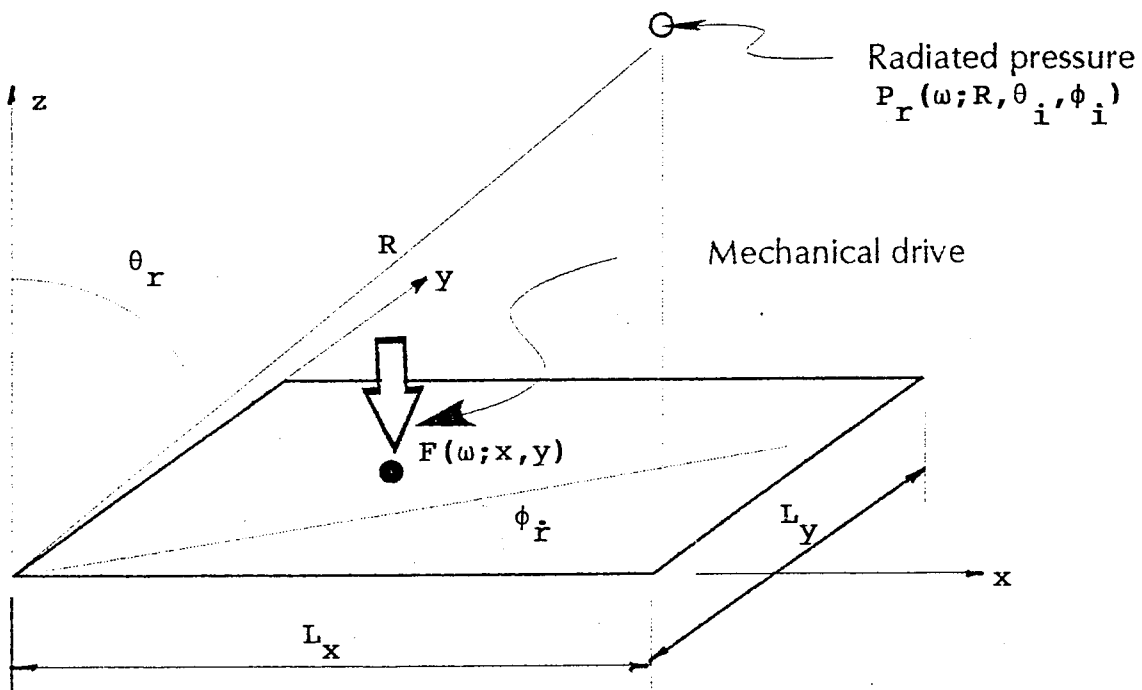


Fig 3b. Mechanically Driven Plate Radiating Sound: Reciprocal Geometry

### 3.1.1 Plate Response To Incident Acoustic Wave

The harmonic displacement of an orthotropic, rectangular, simply supported thin plate to the imposed point pressure  $F(\omega)\delta(x_s)\delta(y_s)$  is given by<sup>15</sup>

$$\tilde{w}(\omega; x, y) = -(4/M)F(\omega) \sum_m \sum_n Y_{mn} \sin k_m x \sin k_m x_s \sin k_n y \sin k_n y_s \quad (10)$$

with  $k_m = m\pi/L_x$ ,  $k_n = n\pi/L_y$ ,

$$Y_{mn} = Y(\omega; k_m, k_n) = \{\omega^2 [1 - (\omega_{mn}/\omega)^2]\}^{-1} \quad (11)$$

$$(\omega_{mn}/\omega)^2 = (k_m/k_{fx})^4 + 2(k_m/k_{fx})^2(k_n/k_{fy})^2 + (k_n/k_{fy})^4$$

$$k_{fx}^2 = [E_x I_x / (1 - \nu^2) \rho_p h \omega^2]^{1/2} = c_{px} r_{gx} / \omega$$

$$k_{fy}^2 = c_{py} r_{gy} / \omega$$

$$c_p = [E / (1 - \nu^2) \rho_p]^{1/2}$$

$$r_g = (I/h)^{1/2}$$

$$M = \rho_p h L_x L_y$$

In the above,  $\rho_p$  is the plating mass density,  $I$  its cross-sectional moment of inertia  $h$  the plate thickness,  $(c_p r_g)_x$  and  $(c_p r_g)_y$  are the products of the compressional speeds in the plating material and the cross-sectional radii of gyration, along the  $x, y$  directions respectively, and  $k_{fx}$  and  $k_{fy}$  are the associated flexural wavenumbers.

For the distributed pressure  $p(\omega; x_s, y_s)$  Eq. 10 serves as an influence function and the displacement becomes

$$\tilde{w}(\omega; x, y) = -(4/M) \sum_m \sum_n A_{mn} Y_{mn} \sin(k_m x) \sin(k_n y) \quad (12)$$

with

$$A_{mn} = \int_0^{L_y} \int_0^{L_x} p(\omega; x', y') \sin(k_m x') \sin(k_n y') dx' dy' \quad (13)$$

Having determined the plate displacement, the corresponding velocity and acceleration may be computed from

$$\dot{v}(\omega; x, y) = -i\omega w(\omega; x, y) \quad (14a)$$

and

$$\ddot{a}(\omega; x, y) = -\omega^2 w(\omega; x, y) \quad (14b)$$

The associated flexural stresses including those evaluated at the outer most plating fibers are

$$\tilde{\sigma}_x = [E_x(h/2)/(1-\nu^2)][\partial^2 w/\partial x^2 + \nu \partial^2 w/\partial y^2] \quad (15a)$$

and

$$\tilde{\sigma}_y = [E_y(h/2)/(1-\nu^2)][\partial^2 w/\partial y^2 + \nu \partial^2 w/\partial x^2] \quad (15b)$$

Specifically, consider the harmonic pressure component of an acoustic plane wave of magnitude  $P_i$  incident on our plate from a simple farfield acoustic source at  $(R, \theta_i, \phi_i)$

$$p_i(\omega; x', y', 0) = P_i \exp[-iks \sin \theta_i (x' \cos \phi_i + y' \sin \phi_i)] \quad (16a)$$

with

$$P_i = \rho \ddot{Q} \exp(ikR)/4\pi R \quad (16b)$$

where  $R$  is range, and  $\ddot{Q}$  the strength (volume acceleration) of the source.

The wave impinges on the plate ( $z=0$ ) and reflects. Using the high frequency asymptotic solution ( $kL_x, kL_y \gg 1$ ) for analytical simplicity, this reflected wave causes a pressure doubling. Therefore, substituting

$$p(\omega; x', y') = 2p_i(\omega; x', y', 0) \quad (17)$$

in Eq. 13,

$$\begin{aligned} A_{mn} &= 2P_i \int_0^{L_y} \int_0^{L_x} \exp[-i(\kappa_x x' + \kappa_y y')] \sin(k_m x') \sin(k_n y') dx' dy' \\ &= 2P_i I_x I_y \end{aligned} \quad (18)$$

with

$$\begin{aligned}
I_x &= [k_m \exp(-i\kappa_x L_x/2)/(k_m^2 - \kappa_x^2)] [\exp(i\kappa_x L_x/2) - \cos(m\pi) \exp(-i\kappa_x L_x/2)] \\
I_y &= [k_n \exp(-i\kappa_y L_y/2)/(k_n^2 - \kappa_y^2)] [\exp(i\kappa_y L_y/2) - \cos(m\pi) \exp(-i\kappa_y L_y/2)] \\
\kappa_x &= k \sin \theta_i \cos \phi_i \\
\kappa_y &= k \sin \theta_i \sin \phi_i
\end{aligned} \tag{19}$$

The impulse response corresponding to any of the above response functions is given by the transform

$$G(t; x, y) = \pi^{-1} \operatorname{Re} \left\{ \int_0^{\infty} \tilde{G}(\omega; x, y) \exp(-i\omega t) d\omega \right\} \tag{20}$$

Using Eq. 20 as the Green's function for an incident wave of arbitrary waveform  $p_i(t)$  the general time domain solutions for our response functions may be computed from either the convolution

$$f(t; x, y) = \int_0^t p_i(t') G(t-t'; x, y) dt' \tag{21a}$$

or the inverse transform

$$f(t; x, y) = \pi^{-1} \operatorname{Re} \left\{ \int_0^{\infty} p_i(\omega) \tilde{G}(\omega; x, y) \exp(-i\omega t) d\omega \right\} \tag{21b}$$

with the frequency spectrum of the incident wave given by

$$p_i(\omega) = \int_0^{\infty} p_i(t) \exp(i\omega t) dt \tag{22}$$

For example, with a classic unit amplitude N-shaped wave of duration  $\tau_0$ ,

$$p_i(t) = (1 - 2t/\tau_0) \quad 0 < t < \tau_0 \tag{23a}$$

the spectrum is

$$p_i(\omega) = (i\omega)^{-1} [2 \exp(i\omega\tau_0/2) \sin(\omega\tau_0/2) / (\omega\tau_0/2) - (1 + \exp(i\omega\tau_0))] \tag{23b}$$

although there are no such restrictions on  $p_i(t)$ .



### 3.1.2 Sound Radiated By Mechanically Driven Plate

Let us now consider the sound radiated by the above plate when it is driven mechanically, as opposed to acoustically (Fig. 3b).

Eq. 10 still holds but here  $F(\omega)$  represents the spectrum of the direct, or mechanical drive, at  $x_s, y_s$ . The far field acoustic pressure radiated to  $(R, \theta_i, \phi_i)$  by this vibration field, is<sup>16</sup>

$$p_r(\omega; R, \theta_i, \phi_i) = -(\omega^2 \rho / 2\pi) \tilde{W}(\omega; \kappa_x, \kappa_y) \exp(ikR) / R \quad (24)$$

where  $\tilde{W}$ , the double spatial Fourier transform of the displacement field, is defined by

$$\tilde{W}(\omega; \kappa_x, \kappa_y) = \int_{L_y}^{L_y} \int_0^{L_x} \tilde{w}(\omega; x, y) \exp[-(\kappa_x x + \kappa_y y)] dx dy \quad (25)$$

In Eq. 24  $R$  is again range,  $\kappa_x, \kappa_y$  are as defined previously in Eq. 19 and as before for consistency (as well as simplicity) we have again invoked the high frequency approximation ( $kL_x, kL_y \gg 1$ ), here by embedding the plate in a rigid baffle (The Kirchhoff approximation). Combining Eqs. 24 and 25

$$p_r(\omega; R, \theta_i, \phi_i) = -(\omega^2 \rho / 2\pi) [\exp(ikR) / R] \int_0^{L_y} \int_0^{L_x} \tilde{w}(\omega; x, y) \exp[-i(\kappa_x x + \kappa_y y)] dx dy \quad (26)$$

or, using Eq. 10

$$p_r(\omega; R, \theta_i, \phi_i) / F(\omega; x_s, y_s) = (4/M)(\omega^2 \rho / 2\pi) [\exp(ikR) / R] \sum_m \sum_n Y_{mn} \int_0^{L_y} \int_0^{L_x} \sin(k_m x') \sin(k_n y') \exp[-i(\kappa_x x' + \kappa_y y')] dx' dy' \sin(k_m x_s) \sin(k_n y_s) \quad (27)$$

We now compare Eq. 27 with the expression previously developed for the structural acceleration in response to the acoustic source (Eq. 14b using Eq. 12 with  $A_{mn}$  defined by Eq. 18 and  $P_i$  by Eq. 16b)

$$\bar{a}(\omega; x, y) / \bar{Q}(\omega; R, \theta_i, \phi_i) = (+/M)(\omega^2 \rho / 2\pi) [\exp(ikR) / R] \sum_m \sum_n \int_0^{L_y} \int_0^{L_x} \sin(k_m x') \sin(k_n y') \exp[-i(\kappa_x x' + \kappa_y y')] dx' dy' \sin(k_m x) \sin(k_n y) \quad (28)$$

We see that the point harmonic acceleration of the plate at  $(x, y)$  to the acoustic source  $\bar{Q}$  at  $(R, \theta_i, \phi_i)$  is reciprocal to the pressure radiated to  $(R, \theta_i, \phi_i)$  by the plate harmonically vibrating in response to the mechanical drive  $F$  at  $(x_s = x, y_s = y)$ , that is,

$$p_r(\omega; R, \theta_i, \phi_i) / F(\omega; x, y) = \bar{a}(\omega; x, y) / \bar{Q}(\omega; R, \theta_i, \phi_i) \quad (29)$$

The harmonic point displacements and velocities may also be determined reciprocally from Eqs. 14. Also, in light of Eq. 20 reciprocity holds in the time domain for impulses, or more generally as long as the force and the acoustic source exhibit the same spectra.

Using superposition, reciprocal relationships may also be developed for distributed rather than point response functions, for example the average acoustically excited plate response is reciprocal to the radiation from a uniformly driven plate. Reciprocal relationships also exist for response functions involving gradients, for example stress (Eqs. 15). However, here reciprocity requires a mechanical drive with a higher order singularity, e.g., a doublet for a moment, etc. This is deemed impractical.

### 3.1.3 Numerical Results

In this section we present numerical results. The geometric, temporal and physical constants are chosen for illustrative purposes but are representative. Unfortunately, even with our elementary model there is a multitude of parameters. They are nondimensionalized as follows for the purpose of generating universal response curves

$$\gamma = L_y / L_x = \text{ratio of plate lateral dimensions}$$

$r_g/L_x = (h/\sqrt{12}L_x) =$  slenderness ratio

$\eta =$  material loss factor

$\nu =$  Poisson's ratio

$(c_p r_g)_x / (c_p r_g)_y =$  ratio of plating stiffnesses along  $x$  and  $y$  axes

$\alpha = \sin^{-1}(1/M) = \theta_i =$  Mach angle, or polar angle of the incident acoustic wave or, reciprocally, of the radiated pressure.

$M = c/U =$  effective Mach number

$\phi_i =$  azimuthal angle of the incident acoustic wave or reciprocally, of the radiated pressure

$c_p/c =$  ratio of plating sound speed to that of air

$\beta^{-1} = c\tau_0/L_x =$  duration of sonic boom normalized by acoustic propagation time over the plate span.

$(x/L_y, y/L_y) =$  normalized coordinates of observer location on plate with acoustic excitation or reciprocally, the mechanical drive location on the radiating plate

$kL_x = \omega L_x/c =$  plate lateral dimension along  $x$  axis

normalized to acoustic wavenumber at frequency  $\omega$  in air

$k_f L_x = (\omega/c_p r_g)_x^{1/2} L_x =$  plate lateral dimension along

$x$  axis normalized to flexural wavenumber at frequency  $\omega$  in plate

$\tau = t/\tau_0 =$  time normalized to pulse duration

$\bar{w} = \tilde{w}/w_{st} =$  plate displacement normalized to the static displacement of (square) plate in response to uniform pressure  $P_i$  ( $w_{st} = 0.049(L_x/h)^3(1-\nu^2)P_i/E$ )

$\bar{\sigma} = \tilde{\sigma}/\sigma_{st} =$  flexural stress normalized to the static stress at (square) plate center in response to the uniform pressure  $P_i$  ( $\sigma_{st} = 0.22(L_y/h)^2(1+\nu)P_i$ )

$\bar{v} = v\tau_0/w_{st} =$  nondimensionalized plate velocity

$\bar{a} = a\tau_0^2/w_{st} =$  nondimensionalized plate acceleration

For our illustrative example we take  $r_g/L = 1.1 \times 10^{-3}$  and

$\beta = 3.53 \times 10^{-2}$  which, for example models a perfect N-wave of  $\tau_0 = 0.2$

sec duration incident on a square uniform plate 2.5cm thick with lateral dimension 2.5m. To approximate solid wallboard construction we further assume  $c_p/c = 4.87$ ,  $\nu = .25$  and somewhat arbitrarily  $\eta = .1$ . For perspective, with these parameters  $\omega_{11}\tau_0 = 3.08$  and therefore the ratio of the period of the fundamental natural frequency of the plate to the pulse duration is  $T_{11}/\tau_0 = 2\pi/\omega\tau_0 \approx 2$ . To determine response time histories the associated frequency spectra have been computed up to  $\omega\tau_0 = 50$  at an increment of  $\Delta\omega\tau_0 = 0.01$ .

In Fig. 4a we plot the computed spectra for the boom itself and the acoustic impulse response of the plate displacement at the center. Also shown as a reference, is the spectral displacement of a simple distributed oscillator (one degree of freedom) when the mass is driven directly by the harmonic pressure with magnitude  $P_i$ .

The oscillator frequency is equal to the fundamental plate frequency and its response has similarly been normalized to its static value. The low frequency plate displacement is 6 dB above that for the oscillator due to the assumed pressure doubling with the acoustic excitation. The corresponding acoustic impulse spectra for the plate velocity, acceleration and flexural stress, all evaluated at the center, have been plotted in Fig. 4b. As with the displacement the (eventual) 6 dB low frequency value for the stress is attributable to pressure doubling. At the higher frequencies, and ignoring oscillations, the acceleration is essentially frequency invariant.

Of particular interest are the velocity and stress spectra. As discussed earlier in Section 2.1, Hunt<sup>3</sup> has shown that for resonant rods and low order resonant beams and plates, the ratio of peak stress to peak velocity is of simple form

$$\tilde{\sigma}_{pk} / \tilde{v}_{pk} \rho_p c_p = K \quad (30)$$

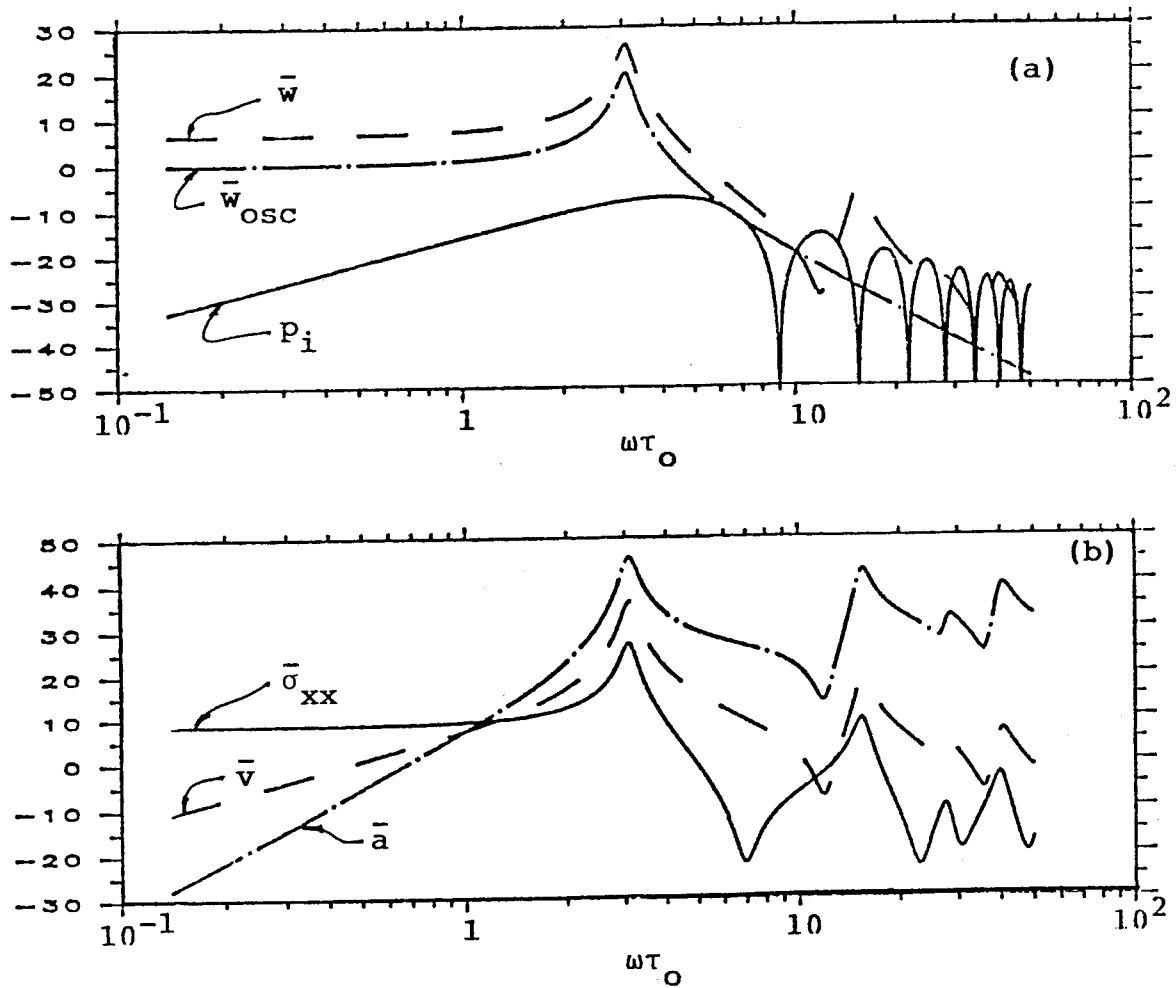


Fig. 4 Sonic Boom and Plate Response Spectra: (a) Sonic boom, plate and oscillator displacement; (b) Flexural stress, velocity and acceleration.

where  $\rho_p$  and  $c_p$  refer to the density and sound speed in the structural element. For a simply supported plate

$$K = \sqrt{3}(1 + \alpha\nu)/4(1 + \alpha^2) \quad (31)$$

With our parameters ( $\alpha = 1, \nu = .25$ )  $K = 1.08$  or  $0.7 \text{ dB}$ . This result is explored in Fig. 5 where the spectra of the stress and the ratio of stress to velocity have been replotted, the latter normalized as follows

$$\tilde{\sigma}/\tilde{v}\rho_p c_p = [4.49\sqrt{12}(r_g/L_x)(1 + \nu)(c_p/c)/\beta]\bar{\sigma}/\bar{v} \sim 2.98\bar{\sigma}/\bar{v} \quad (32)$$

or

$$20 \log |\tilde{\sigma}/\tilde{v}\rho_p c_p| = 9.5 + 20 \log \bar{\sigma} - 20 \log \bar{v}$$

Also plotted in Fig. 5 is Eq. 31. As expected, the exact solution is well predicted by Eq. 31 at the lower natural frequencies of our plate where the stress peaks, although the comparison may be poor elsewhere.

Computed time histories are shown in Figs. 6 and 7a with that of the boom as a reference. The long time oscillations (ringing) by and large correspond to the fundamental plate frequency. Hunt's relationship between stress and velocity is once again verified in the time domain where we see that the ratio of  $\bar{\sigma}_{pk}/\bar{v}_{pk} = 2.4/6.3 = 0.38$  or  $-8.4 \text{ dB}$  and therefore  $\tilde{\sigma}_{pk}/\tilde{v}_{pk}\rho_p c_p \sim 1.13$  or  $1 \text{ dB}$  (vs  $0.7 \text{ dB}$ ). Finally, in Fig. 7b we show stress and velocity and time histories for an orthotropic plate and oblique incidence/radiation. Here we compute  $\tilde{\sigma}_{pk}/\tilde{v}_{pk}\rho_p c_p \sim 0.75$ .

### 3.2 THE DIFFRACTED AIRBORNE PATH

In practice structural elements such as individual windows and walls, may often be shadowed from the boom and also baffled by surrounding structure. Structural-acoustic reciprocity allows for both of these phenomena. This is illustrated below for the example shown in Fig. 8 using a coupled finite element-boundary element (FE/BE) numerical approach to the solution of the

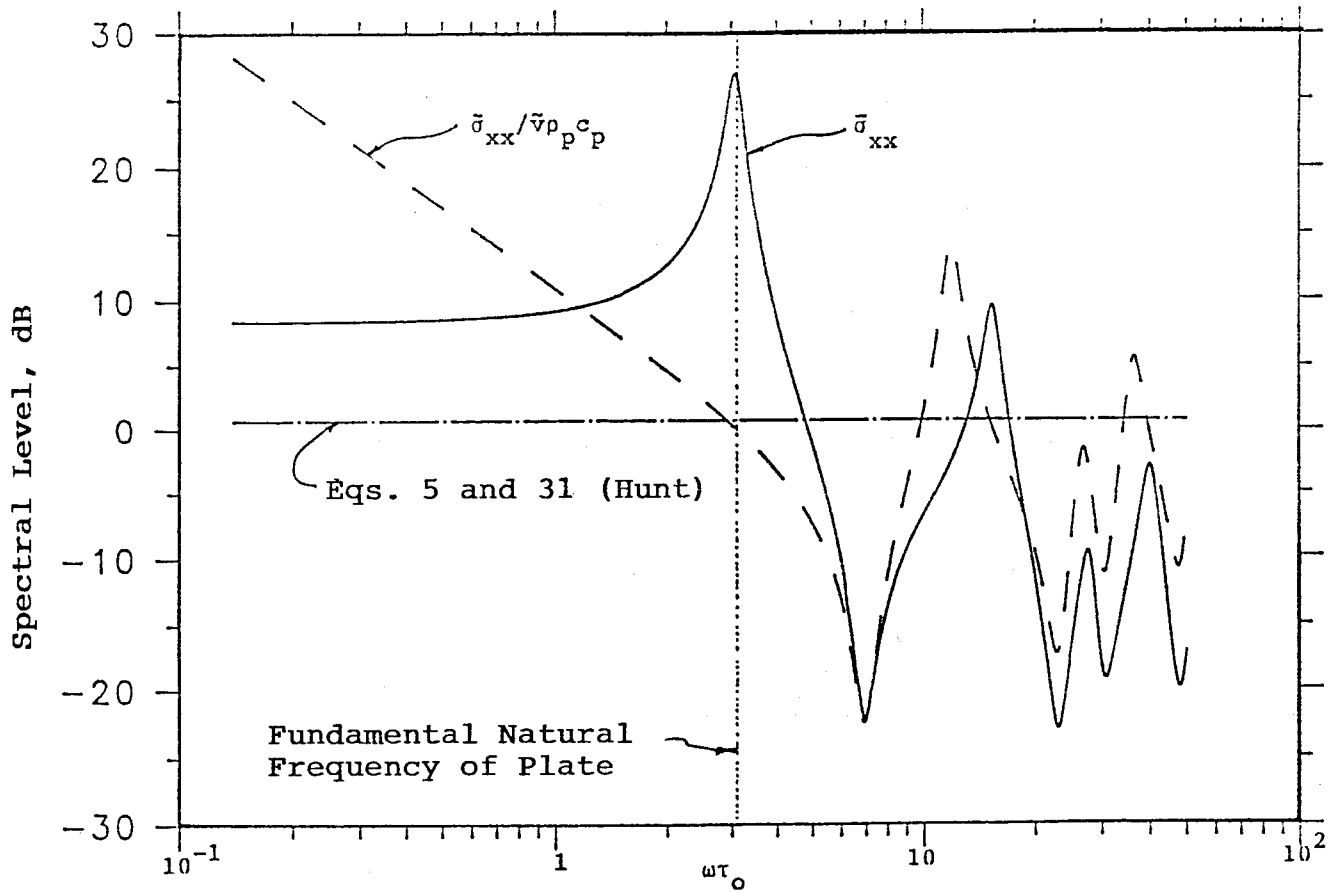


Fig. 5 Flexural Stress Levels and Ratio of Stress to Velocity Spectral Levels at Plate Center vs Frequency.

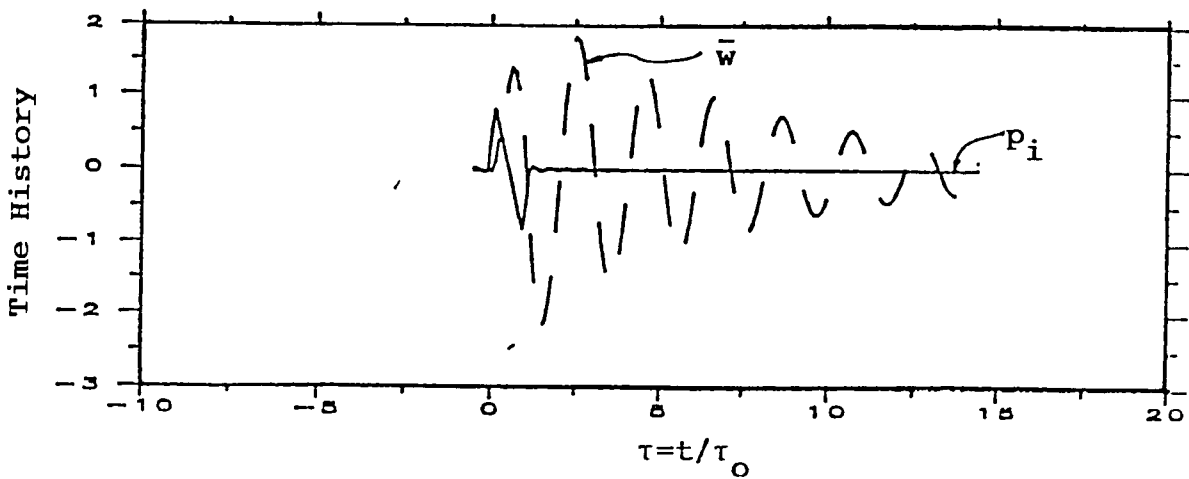
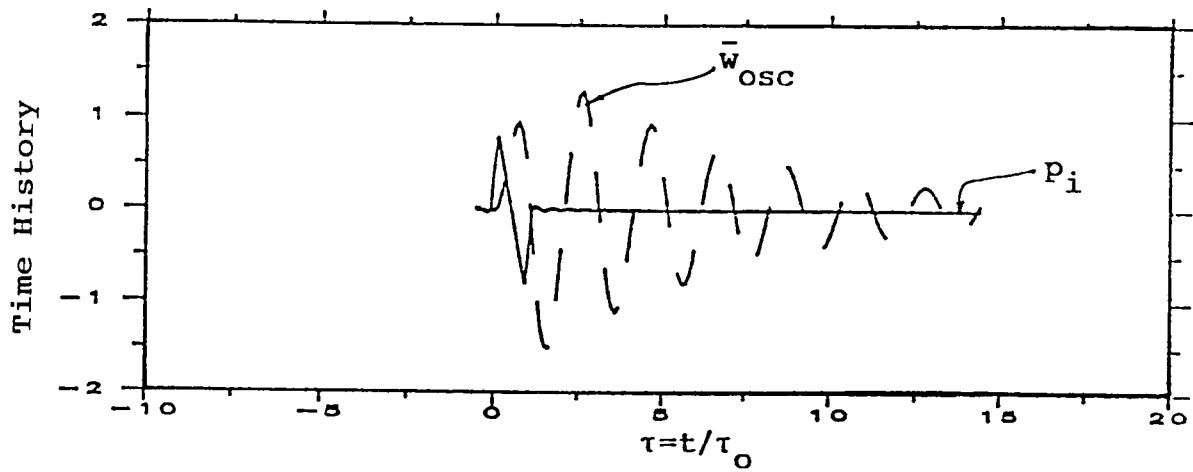


Fig. 6 Time Histories for Sonic Boom Pressure and Plate and Oscillator Displacements.



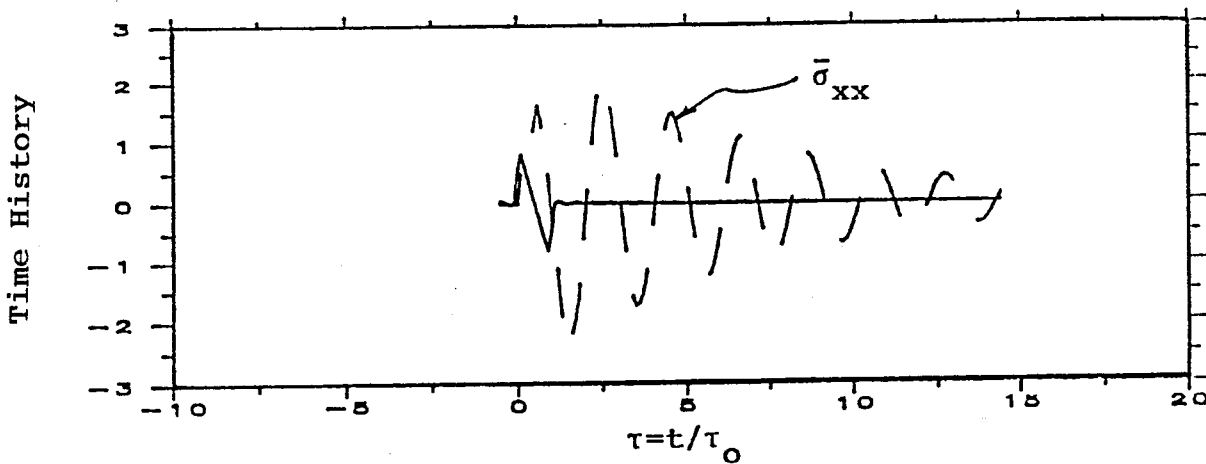
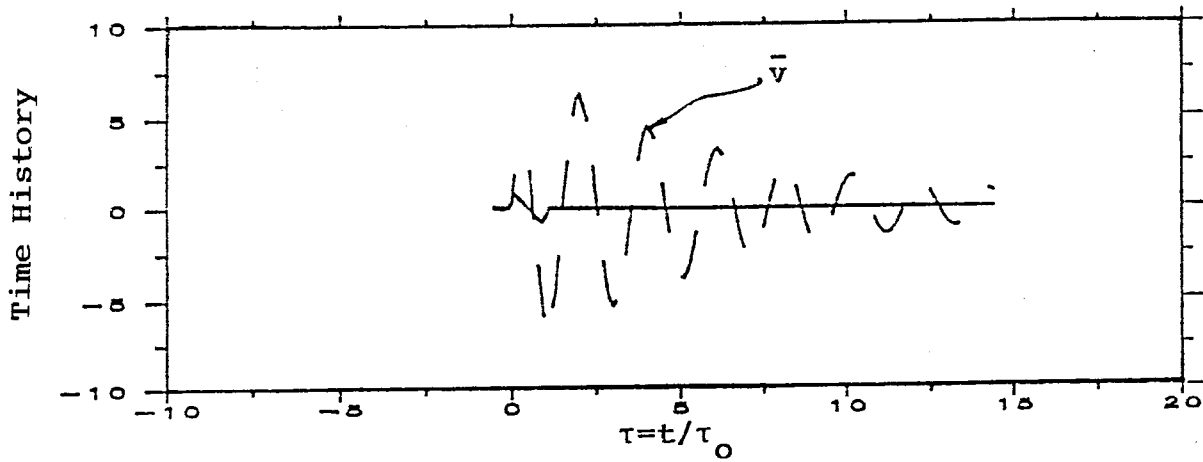


Fig. 7a Time Histories for Sonic Boom Pressure and Plate Velocity and Stress.

$$(\theta_i = \phi_i = 0, (r_g)_y / (r_g)_x = 1: (\bar{\sigma} / \bar{v} \rho c)_P = 2.98 \quad \bar{\sigma} / \bar{v} \sim 1.15$$

$P_{P \max}$

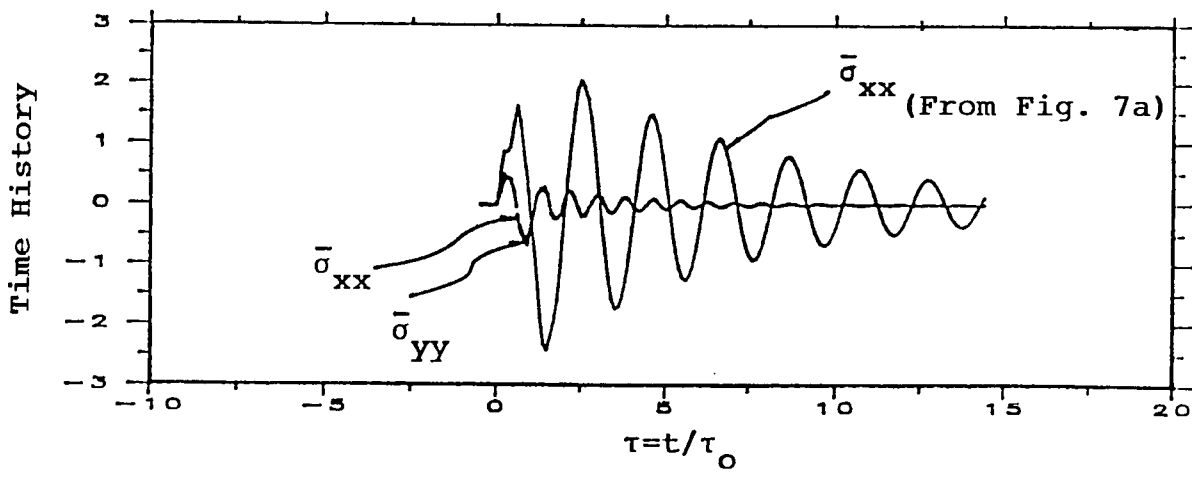
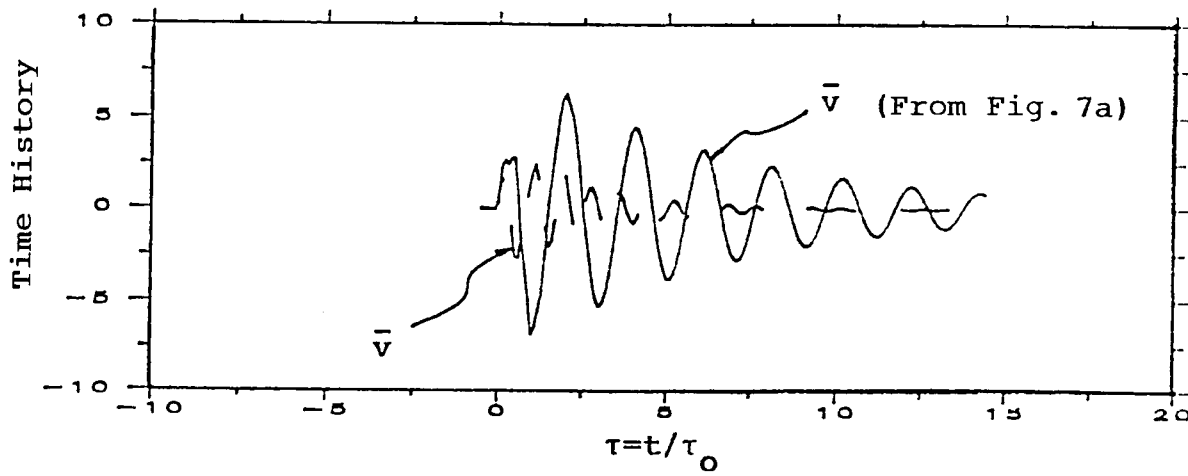


Fig. 7b Time Histories for Sonic Boom Pressure and Plate (center) Velocity and Stress.

$$(\theta_i = \phi_i = 45^\circ, (r_g)_y / (r_g)_x = 4: (\tilde{\sigma} / \tilde{v} \rho_p c_p)_{\max} = 2.98 \bar{\sigma} / \bar{v} \sim 0.75$$

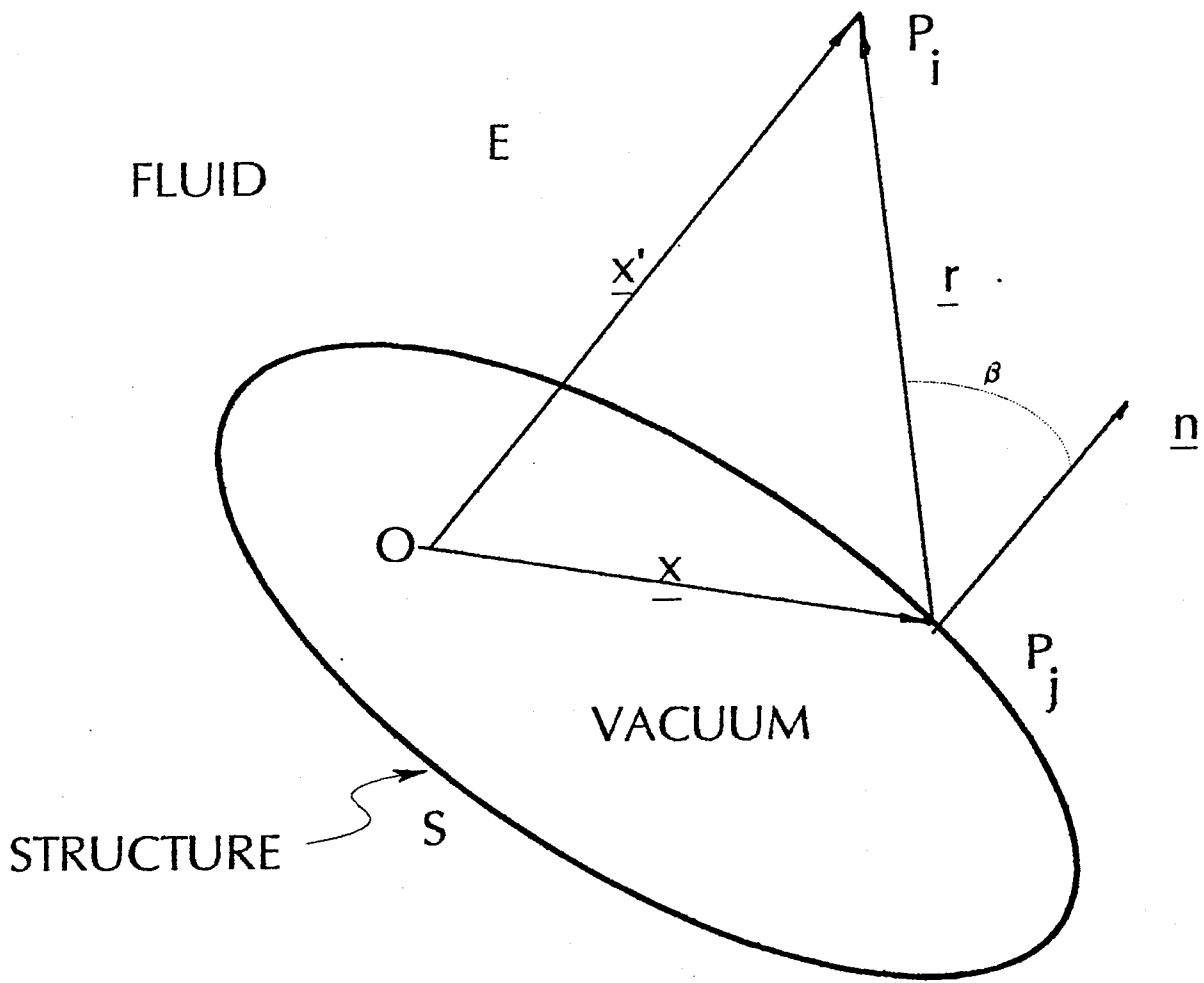


Fig 8. Notation For Helmholtz Integral Equation

Helmholtz integral equation. The example also illustrates at the currently available power of state-of-the-art general purpose FE/BE computer codes to model complex structural acoustic interactions.

### 3.2.1 The Helmholtz Integral Equation

The dynamic behavior of a structure embedded in an acoustic medium can be described by the matrix equation<sup>17</sup>

$$Z\dot{u} = F - GAP \quad (33)$$

where  $Z$  is the structure's mechanical impedance,  $\dot{u}$  is the velocity vector,  $F$  is the mechanical force acting on the body,  $G$  and  $A$  are the geometry matrices of the surface normals and areas defining the fluid-structure interface, and  $P$  is the fluid pressure acting on the body. The structure's mechanical impedance  $Z$  is defined as a function of frequency as

$$Z = F/\dot{u} = (i\omega M + D + K/i\omega) \quad (34)$$

where  $M, D,$  and  $K$  are the mass, damping and stiffness matrices of the structure.

The fluid behavior is described by the Helmholtz integral equation

$$\int p(\underline{x}) \frac{\partial D(\underline{r})}{\partial \underline{n}} dS - \int_S q(\underline{x}) D(\underline{r}) dS = \begin{cases} p(\underline{x}')/2 - p_I, & \underline{x} \text{ on } S \\ p(\underline{x}') - p_I, & \underline{x} \text{ on } E \end{cases} \quad (35)$$

where the vectors  $\underline{x}, \underline{r}, \underline{x}'$ , and  $\underline{n}$  along with the geometry are described in Fig. 8,  $D(\underline{R})$  is the Green's function, and  $q(\underline{x})$  is the normal pressure gradient. These variables are defined in the equations:

$$D(\underline{r}) = e^{-ik\underline{r}} / 4\pi\underline{r}, \quad (36)$$

$$q(\underline{x}) = \partial p(\underline{x}) / \partial \underline{n} = -i\omega\rho \dot{u}_n(\underline{x}) \quad (37)$$

$$\partial D(\underline{r}) / \partial \underline{n} = \frac{e^{-ikr}}{4\pi r} (ik + 1/r) \cos\beta \quad (38)$$

The quantity  $\dot{u}_n$  in Eq. 37 is the normal velocity on the surface,  $S$ , while the far-field angle  $\beta$  relative to the surface normal is defined in Fig. 8. Substitution of Eqs. 36, 37, and 38 into the form of Eq. 35 valid for points on  $S$  (taken to be the surface of the structure) yields the integral equation

$$\frac{1}{2}p(\underline{x}') - \int_S p(\underline{x}) \frac{e^{-ik\underline{r}}}{4\pi\underline{r}} \left( ik + \frac{1}{r} \right) \cos\beta dS = i\omega\rho \int_S \dot{u}_n(\underline{x}) \frac{e^{-ik\underline{r}}}{4\pi\underline{r}} dS + p_i \quad (39)$$

Numerical integration of the surface integrals allows Eq. 39 to be cast into a discrete matrix equation of the form

$$EP = C\dot{u}_n + P_i \quad (40)$$

The normal velocities on the structure are obtained from the  $G$  matrix by the equation

$$\dot{u}_n = GT\dot{u}. \quad (41)$$

Eqs. 33, 40, and 41 can be combined to give

$$HP = Q + P_i, \quad (42)$$

where  $H = E + CG^T Z^{-1}GA$  and  $Q = CG^T Z^{-1}F$ .

Eq. 42 is the coupled matrix equation for the structure and the fluid valid on the surface of the structure which is solved to give the pressure acting on the surface. The normal velocity  $\dot{u}_n$  is then obtained from Eqs. 33 and 41. Substituting these quantities into Eq. 35 provides the solution for the far-field pressure.

Lastly, we note that the Helmholtz integral equation is singular at a discrete set of "forbidden" frequencies. These frequencies correspond to the acoustic resonances of the interior cavity. To alleviate this problem, NASHUA introduces "CHIEF points"

(combined Helmholtz Integral Equation Formulation<sup>18</sup>) to the interior volume. These points, together with the interior Helmholtz integral equation, are used to generate a number of additional equations that impose needed constraints to the system.

### 3.2.2 Illustrative Example

Our example is of a cubic structure resting on a rigid ground plane (Fig. 9a). All walls of the structure save one are assumed immovable. Centrally embedded in the otherwise rigid remaining wall is a square "window" modelled as an isotropic simply supported plate. The window side length ( $L_w$ ) is one third that of the cube ( $L$ ) and its slenderness ratio is  $r_g/L_w = 4.8 \times 10^{-3}$ . It is made of glass ( $c_p/c = 15.5$ ,  $\nu = 0.3$  and somewhat arbitrarily,  $\eta = 10^{-6}$ ). For computational convenience the interior air space is ignored. The finite element model of the structure is created using the finite element program COSMIC NASTRAN. The formulation of the Helmholtz boundary elements and its interface with NASTRAN is performed using the NASHUA code<sup>17</sup>.

To numerically demonstrate reciprocity the window will be driven acoustically and mechanically and the appropriate results compared in the spectral domain for nondimensional frequencies  $0.1 < kL < 1.2$ . A computer plot of our model is shown in Fig. 9b. Because the structure and the applied loads are symmetric only half the structure is modeled. Highlighted in the plot is the plane of symmetry, the ground plane, and the window. Each element measures roughly  $1/8$  of an acoustic wavelength at  $kL = 12$ .

$(R, \theta, \phi)$

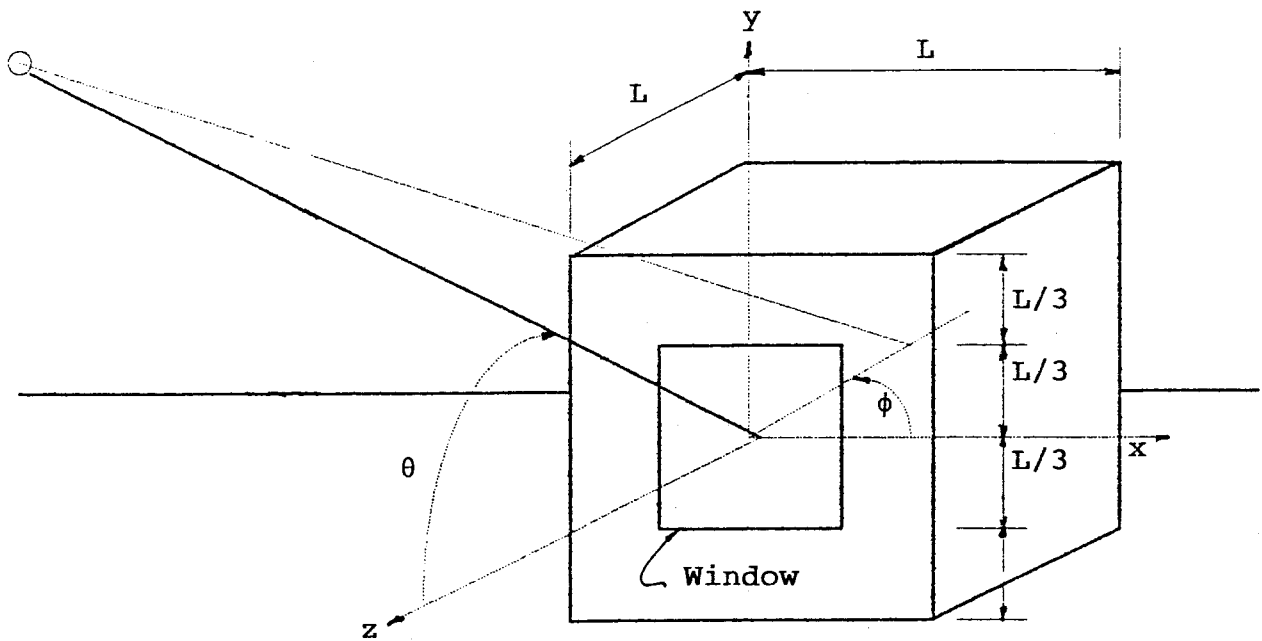


Fig 9a. Elastic Window Embedded In An Otherwise Rigid Walled Cubic Structure Resting On A Rigid Ground Plane

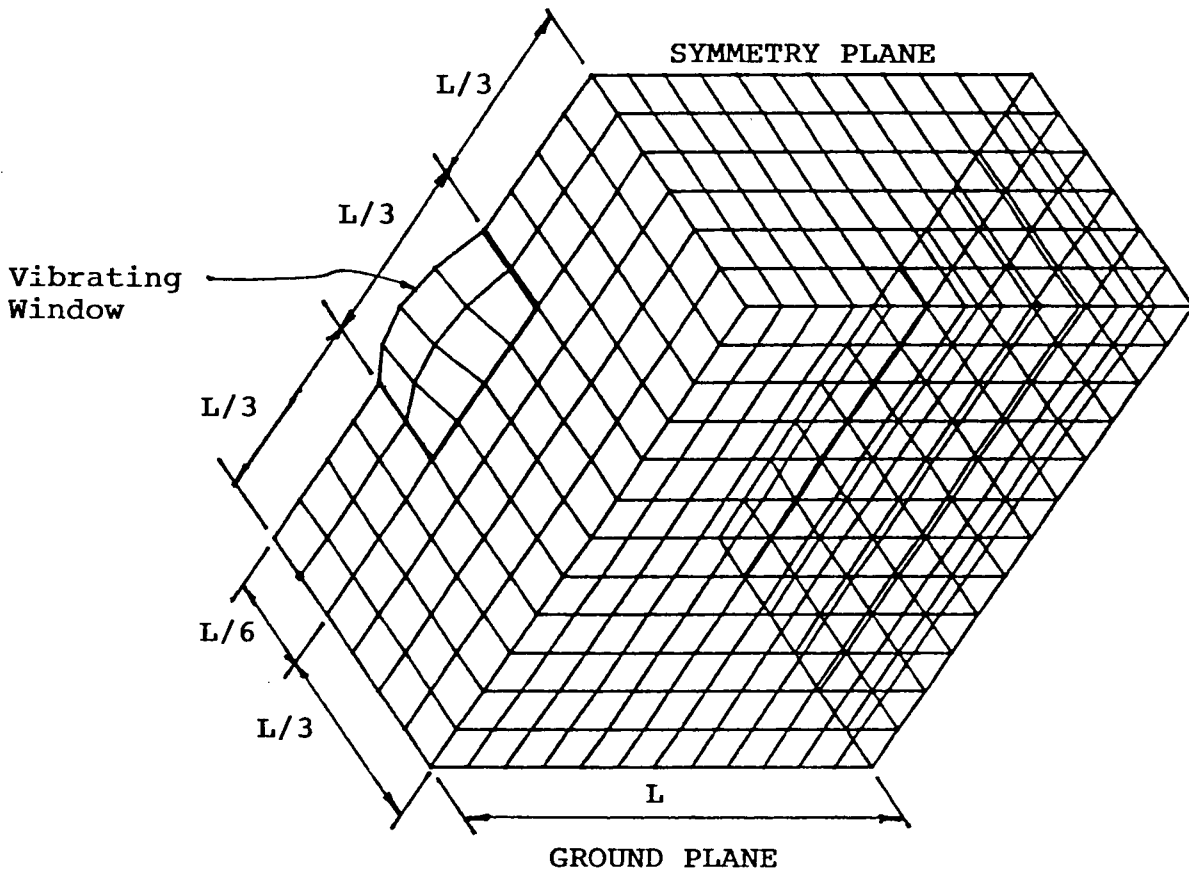


Fig. 9b Sketch of Window Response Computed Using FE/BE Computer Code.



### 3.2.3 Numerical Results

First, for our reciprocal calculation we apply a concentrated normal force to the center of the window and compute the radiated pressure at a number of receiver locations assumed to be in the far field. Specifically, the pressure is calculated at  $(R,0,0)$ ,  $(R,\pi,0)$ ,  $(R,\pi/2,\pi/2)$  and  $(R,\pi/2,0)$  corresponding to receivers in front of, in back of, above, and to the side of the window and where  $R(=1m)$  is a reference far field range. Results are plotted in Fig. 10. As a reference with  $L=3L_w=2.28m$  and assuming  $c=340m/s$ ,  $kL=1.0$  corresponds to 24. Hz. The radiated pressure has been normalized to that radiated in the absence of the rigid structure but in the presence of the rigid ground plane.

At small values of  $kL$  the driven window behaves as a monopole source radiating omnidirectionally. At the receiver located above the window destructive interference from ground reflections is evident beginning at  $kL=\pi$  where the path difference between the direct and the ground reflected waves first measures one-half acoustic wavelength in air. The baffling effect of the rigid walls surrounding the window accounts for up to a 10 dB difference in front to back radiation levels. Of particular interest is the fact that the maximum radiated levels actually exceed the 6 dB increase associated with an acoustic source in a baffle of infinite extent.

For our direct calculation we now compute the velocity at the center of the window for an incident plane wave. Corresponding to the earlier receiver locations, the orientation of our plane wave is defined by a far field acoustic source located at spherical coordinates  $(R,0,0)$ ,  $(R,\pi,0)$  and  $(R,\pi/2,\pi/2)$ , the fourth location omitted for computational convenience.

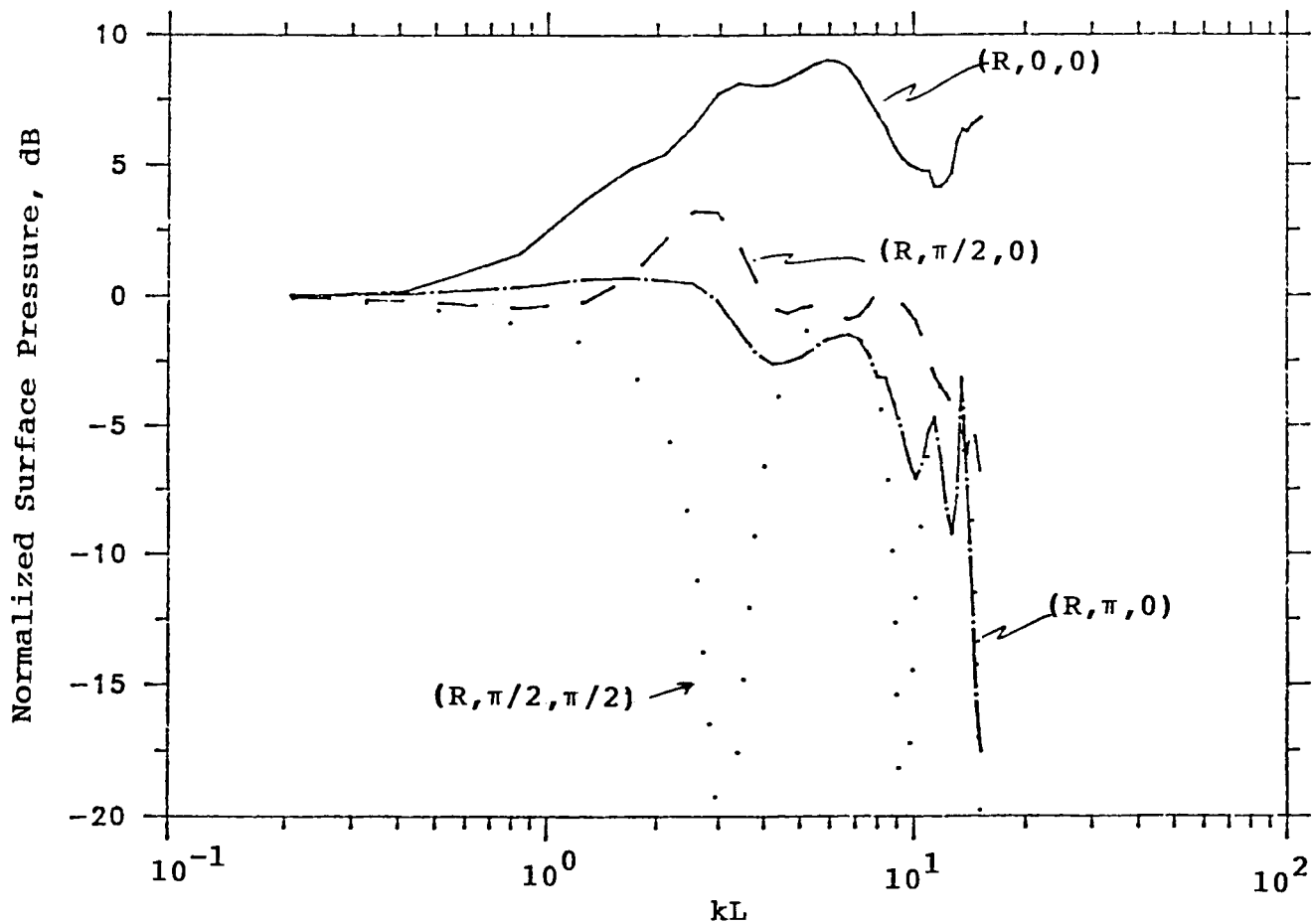


Fig. 10 Effect of Rigid Wall Baffle on Window Surface Pressure Normalized To Free Field Incident Pressure Level.

Direct and reciprocal calculations are compared in Figs. 11a,b and c, the latter renormalized to demonstrate reciprocity as per Eq. 7 (or 29). Differences, which may be attributed to the discretization process and the accuracy of our solution to the simultaneous equations given by Eq. 42, are generally imperceptible. To highlight the diffraction effect itself, we plot in Fig. 12 our direct calculation of the (normalized) window center velocity for the ground level source placements corresponding to marginally supersonic flyovers, i.e.,  $M \sim 1$  oriented such that the window is illuminated, shadowed and grazed by the incident boom.

Finally, we note that the above coupled FE/BE approach can have easily been used to analyze a more complex geometry and structure. For example, the walls need not have been rigid nor in the shape of a cube. The window could also have been of any shape and of any construction allowing linear viscoelastic or structural modelling. This could include provisions for studded, composite, or brick and mortar walls and brick and brace attachments.

### 3.3 THE SEISMIC PATH

A sonic boom induced acoustic field impinges on the ground plane as well as on man-made structures. Generally, due to the large impedance mismatch, this field is almost completely reflected from the plane with little energy coupled into the ground. The exception is at "coincidence" where the wavenumber of the airborne acoustic wave projected on the plane matches that of a characteristic wave propagating in the ground. In particular, coupling may be strong at coincidence with Rayleigh surface waves which propagate at close to the ground shear speed and remain trapped near the surface. As with the airborne pressure field this coupled ground-borne energy may reradiate, excite structures and potentially cause unacceptable noise levels and/or damage.

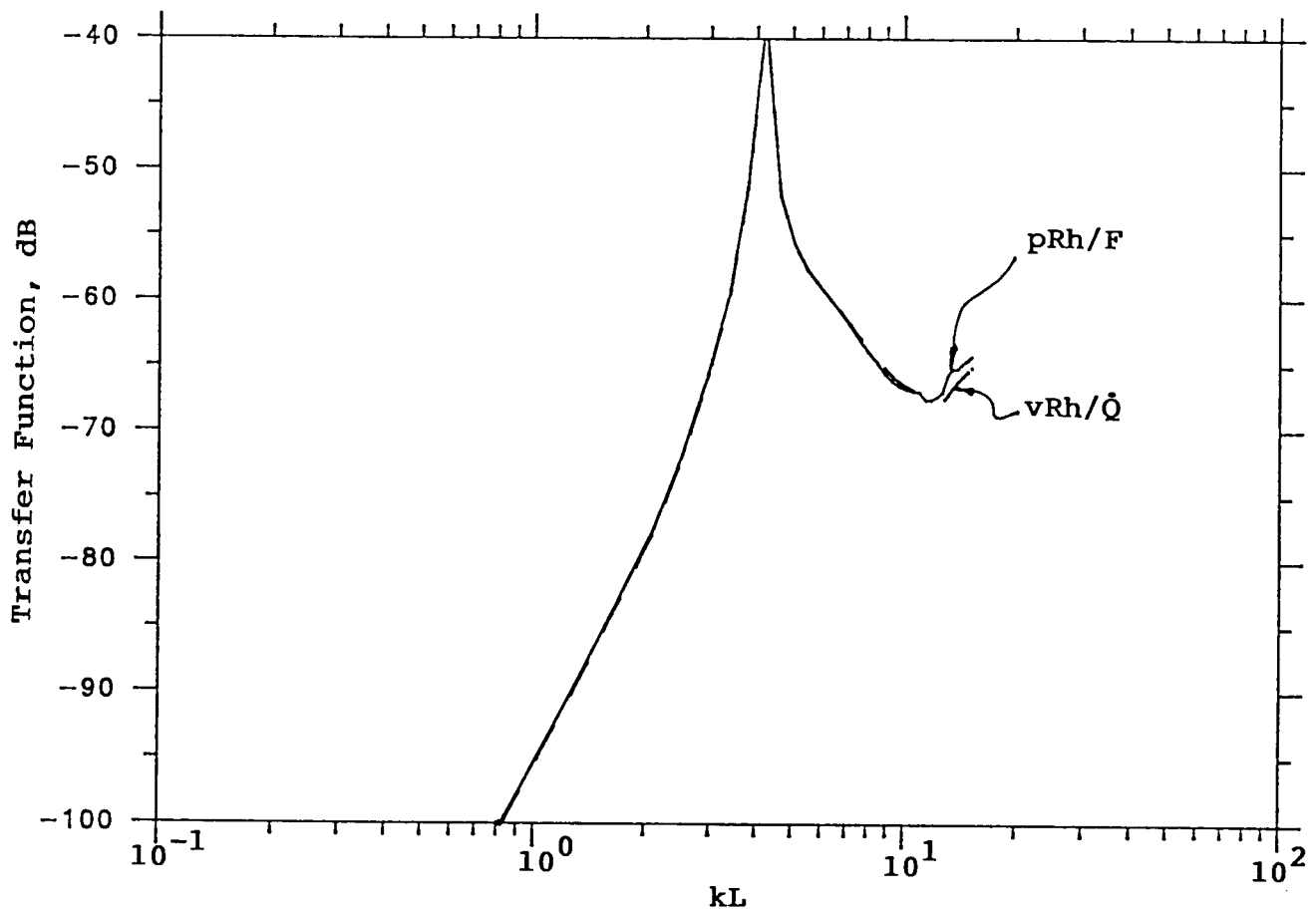


Fig. 11a Transfer Function for Window Response To Acoustic Wave Computed Directly and Reciprocally: Window Illuminated (R,0,0).

Transfer Function, dB

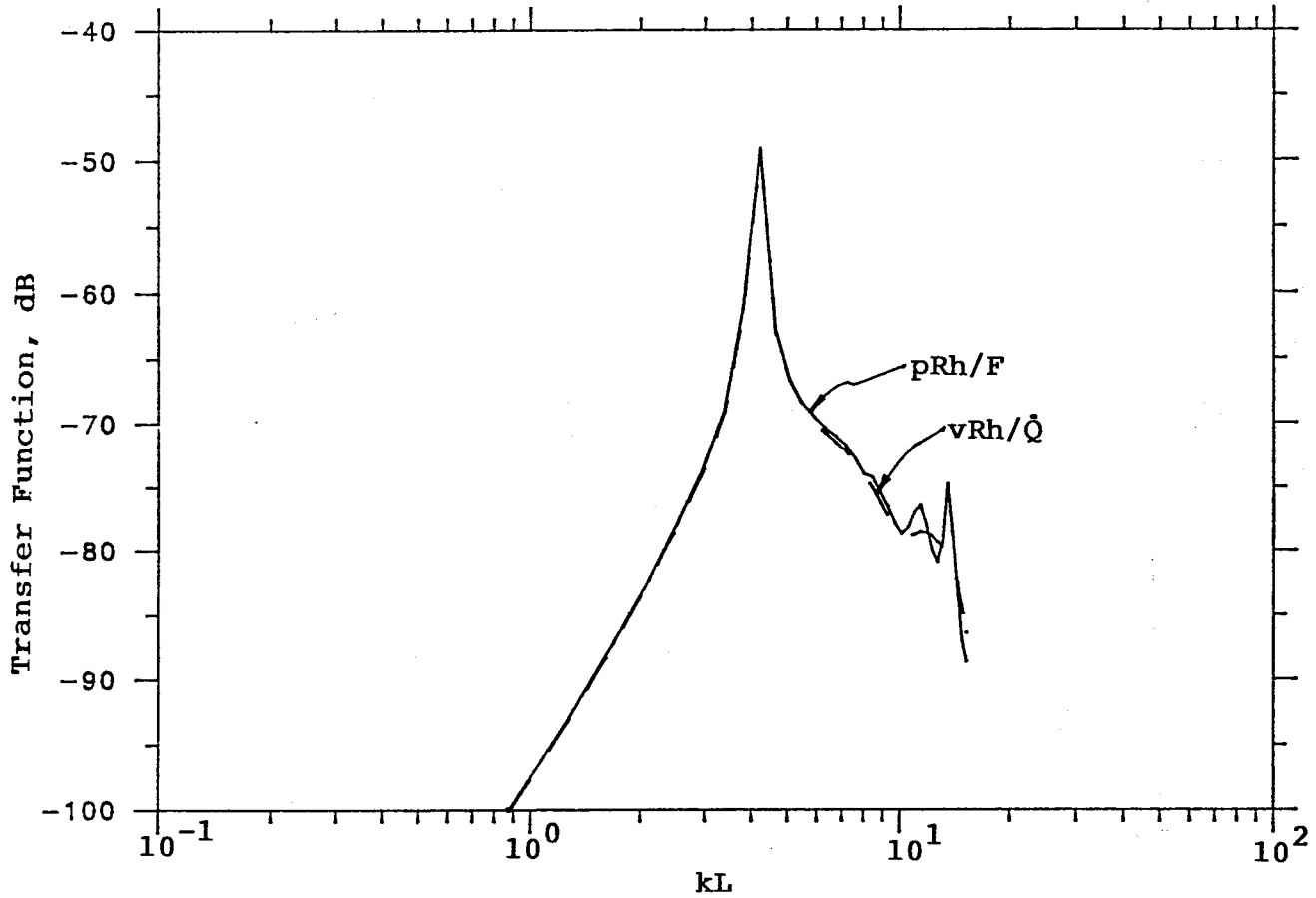


Fig. 11b Transfer Function For Window Response To Acoustic Wave Computed Directly and Reciprocally: Window in Shadow ( $R, \pi, 0$ ).

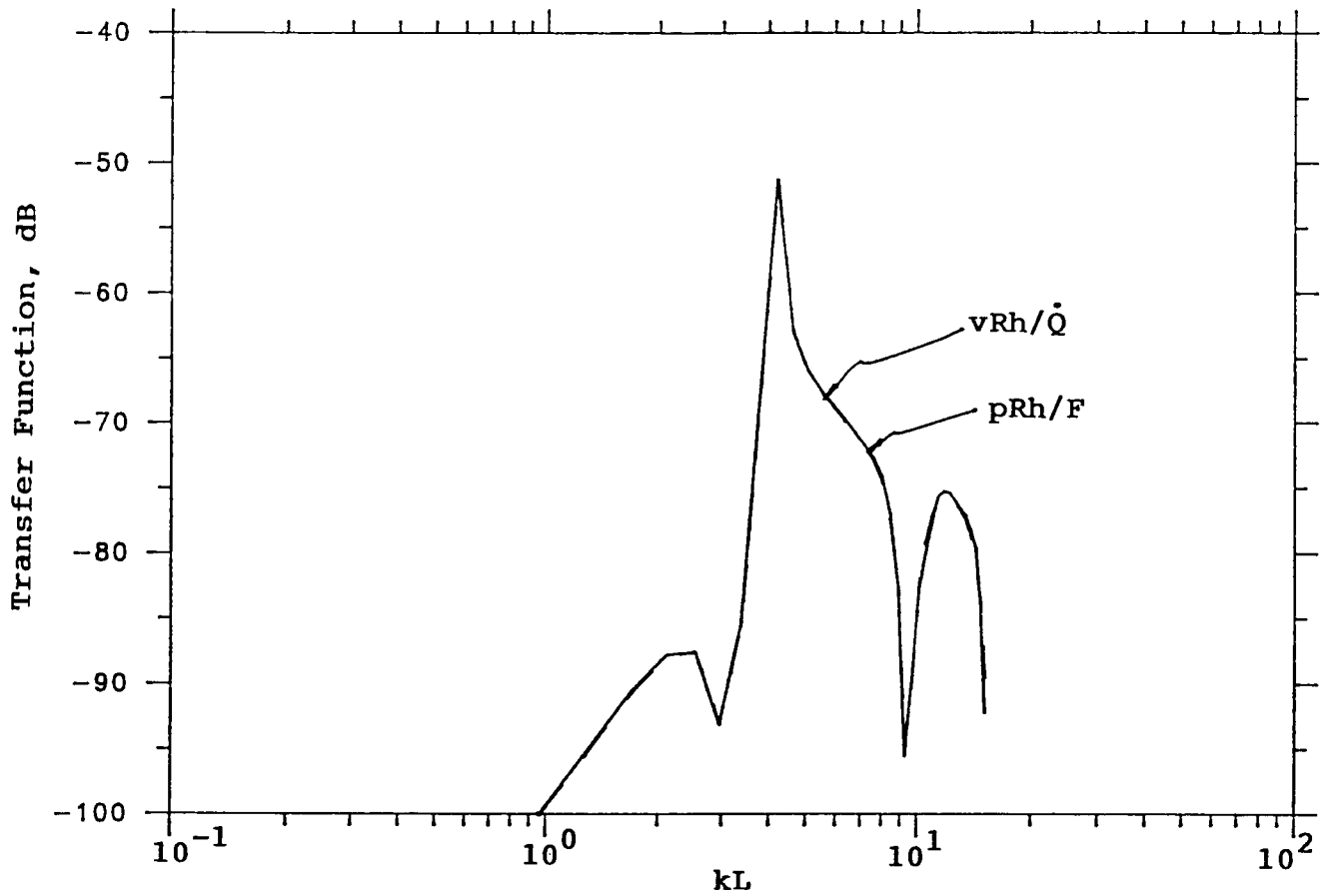


Fig. 11c Transfer Function For Window Response to Acoustic Wave Computed Directly and Reciprocally: Wave Incident From Above ( $R, \pi/2, \pi/2$ ).

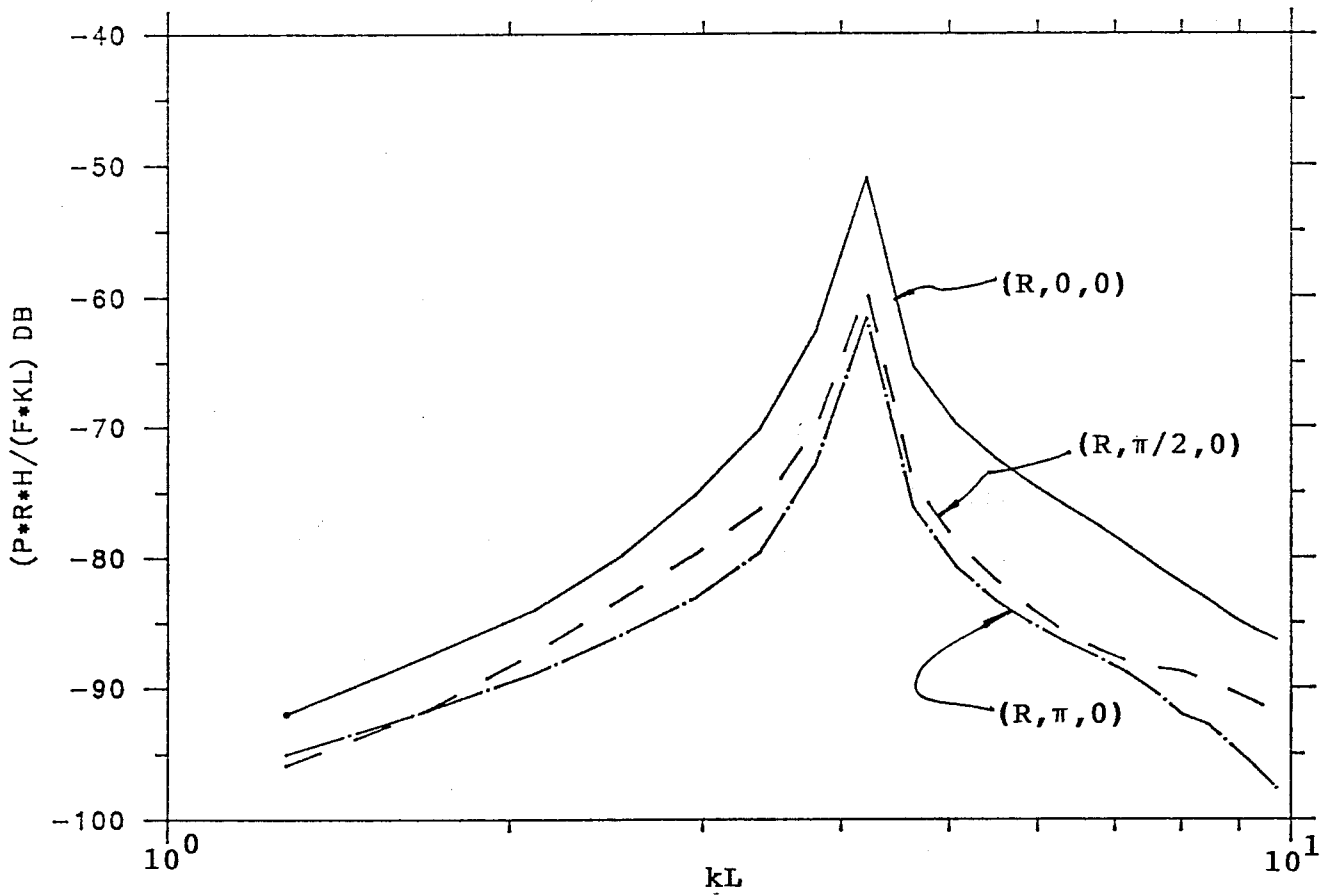


Fig. 12 Normalized Window Velocity Per Unit Incident Pressure For three (M-1) Flyover Orientations (— Illuminated, — — Grazing, —. — Shadow).

In practice however this path appears to be relatively weak.<sup>19</sup> Nevertheless, it also satisfies reciprocity as is demonstrated below, assuming the incident field to be acoustic and the ground a linear viscoelastic medium.

For our illustrative purposes, we consider the situation pictured in Fig. 13a. As before, a distant acoustic source of volume velocity  $\dot{Q}$ , or volume acceleration  $\ddot{Q}$ , generates an effectively plane acoustic wave in the far field. Letting  $\phi_i = 0$ ,

$$p_i(\omega; x, z) = P_i(\omega; x, z) \exp\{ik[(x - x_s)\sin\theta + (z - z_s)\cos\theta]\} \quad (45)$$

with

$$P_i(\omega; x, z) = -i\omega\rho\dot{Q}(\omega; x_s, z_s)/4\pi R_s(|x - x_s|, |z - z_s|)$$

Evaluating Eq. 45 on the ground plane

$$p_i(\omega; x, 0) \Rightarrow P_i(\omega; x, 0) \exp\{ik[(x - x_s)\sin\theta - z_s\cos\theta]\} \quad (46)$$

The reflected (plane) wave is given by<sup>20</sup>

$$p(\omega; x, z)/P_i(\omega; x, 0) = \gamma \exp\{ik[(x - x_s)\sin\theta - (z - z_s)\cos\theta]\} \quad (47)$$

with

$$\gamma = (\bar{Z}(k_x)\cos\theta - 1)/(\bar{Z}(k_x)\cos\theta + 1) \quad (48)$$

and

$$\begin{aligned} \bar{Z}(k_x) = Z(k_x)/\rho c = (\rho_g c_d/\rho c) \{ [1 - 2(k_x/k_s)^2]^2 + 4(k_d/k_s)(k_x/k_s)^2 \\ [1 - (k_x/k_s)^2]^{1/2} [1 - (k_x/k_d)^2]^{1/2} \} / [1 - (k_x/k_d)^2]^{1/2} \end{aligned} \quad (49)$$

where

$$k_x = k \sin\theta$$

$$k_d = \omega/c_d$$

$$k_s = \omega/c_s$$

In Eq. 49  $\rho_g$  is the ground density and  $c_d$  and  $c_s$  are the dilatational and shear ground speeds. The total (normalized) pressure is

$$p_i(\omega; x, z)/P_i(\omega; x, 0) = [P_i(\omega; x, z) + p(\omega; x, z)]/P_i(\omega; x, 0) \quad (50)$$

which evaluated at  $z = 0$



Fig 13a. Direct Model of Insonified Elastic Ground Plane Covering Elastic Half Space

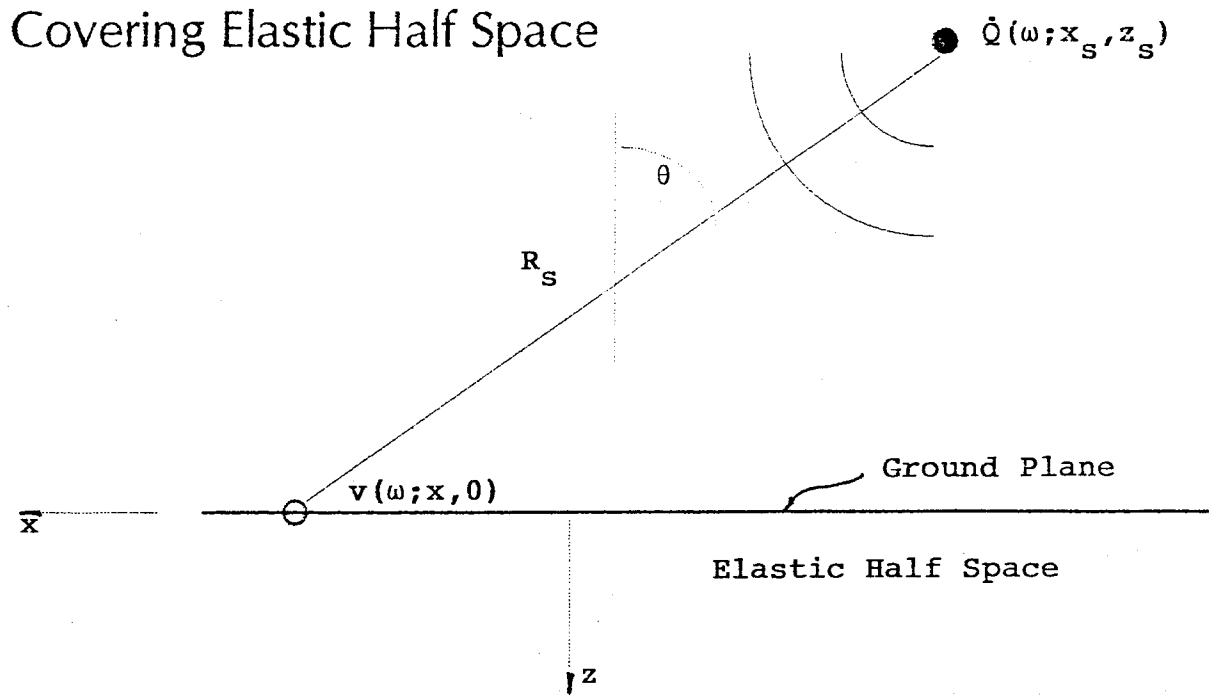
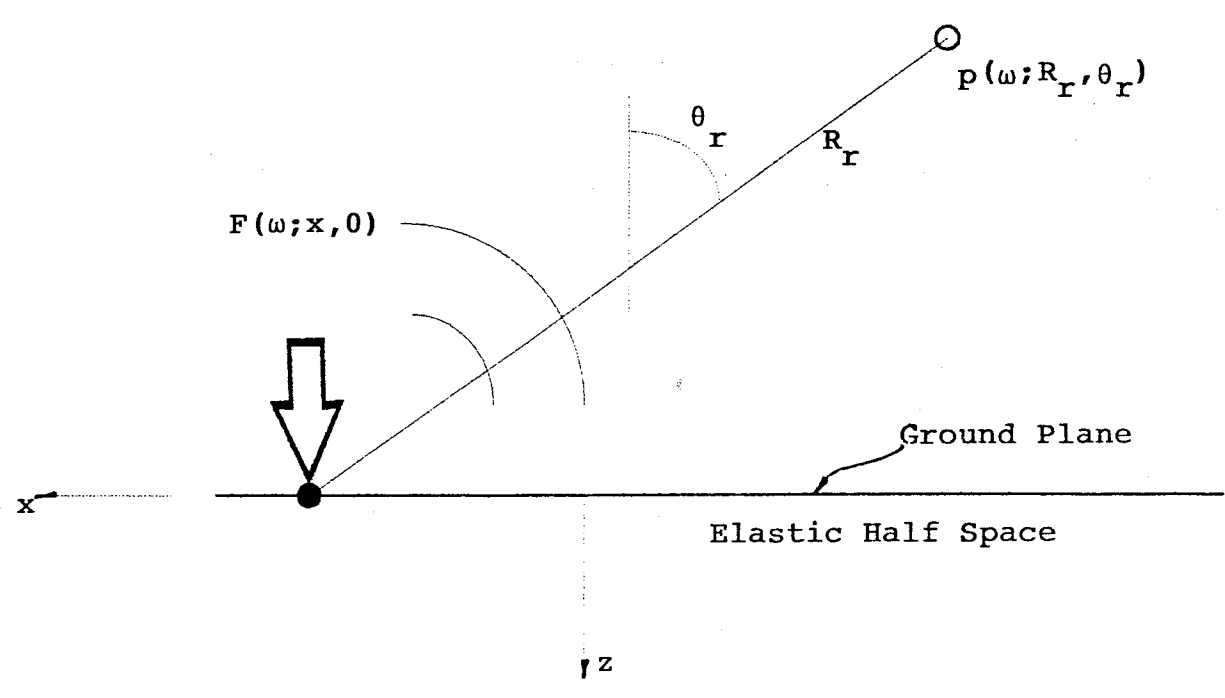


Fig 13b. Reciprocal Model of Sound Radiated by Mechanically Driven Ground Plane



$$\Rightarrow \{2\bar{Z}(k_x)\cos\theta/[\bar{Z}(k_x)\cos\theta+1]\}\exp\{ik[(x-x_s)\sin\theta+z_s\cos\theta]\} \quad (51a)$$

$$-2\exp\{ik[(x-x_s)\sin\theta+z_s\cos\theta]\} \quad \bar{Z}\cos\theta \gg 1 \quad (51b)$$

The associated normal particle velocity at ground level is

$$\rho cv(\omega;x,0)/P_i(\omega;x,0) = p_i(\omega;x,0)/P_i(\omega;x,0)\bar{Z} \quad (52a)$$

or

$$\rho cv(\omega;x,0) = -i\omega\rho\dot{Q}(\omega;x_s,z_s)[\cos\theta/(\bar{Z}(k_x)\cos\theta+1)]e^{ikR_s}/2\pi R_s \quad (52b)$$

Now consider the reciprocal situation. As is the case in a free field, acoustic reciprocity allows one to switch source and receiver

$$p_i(\omega;x,z)/\dot{Q}(\omega;x_s,z_s) = p_i(\omega;x_s,z_s)/\dot{Q}(\omega;x,z) \quad (53)$$

In addition, for the reciprocal equivalent to the acoustically induced seismic motion, consider Fig. 13b. A compact normal force ( $F$ ) is applied to the ground surface at  $(x,0,0)$ . The associated axisymmetric surface velocity may be expressed in terms of its radial wavenumber spectrum<sup>21</sup>

$$v(\omega;r) = \int_0^\infty \tilde{v}(\omega;k_r)J_0(k_r r)k_r dk_r \quad (54)$$

with

$$\tilde{v}(\omega;k_r) = (F/2\pi)/[Z(k_r)+z_a(k_r)] \quad (55)$$

where the wavenumber transformed acoustic impedance is given by

$$z_a(k_r) = \rho c/[1-(k_r/k)^2]^{1/2}$$

This transformed velocity also defines the far field radiated pressure,<sup>22</sup>

$$\begin{aligned} p(\omega;R_r,\theta_r) &= -\omega\rho\tilde{v}(\omega;k\sin\theta_r)e^{ikR_r}/R_r \\ &= -i\omega\rho F/[\bar{Z}(k\sin\theta)+1]e^{ikR_r}/2\pi R_r \end{aligned} \quad (56)$$

Comparing Eqs. 52b and 56 we arrive at the reciprocal relationship

$$v(\omega;x,0)/\dot{Q}(\omega;R_s=R_r) = a(\omega;x,0)/\dot{Q}(\omega;R_s=R_r) = p(\omega;R_r)/F(\omega;x,0) \quad (57)$$

Finally, from Eq. 49 we note that since  $\rho_g c_d / \rho c \gg 1$ ,  $\bar{Z} \gg 1$  and the ground is essentially impenetrable except when

$$[1 - 2(k_x/k_s)^2]^2 + 4(k_d/k_s)(k_x/k_s)^2 [1 - (k_x/k_s)^2]^{1/2} [1 - (k_x/k_d)^2]^{1/2} = 0 \quad (58)$$

This is the Rayleigh wave coincidence condition. In contrast, at dilatational wave coincidence,  $k_x/k_d = 1$ , the impedance becomes infinite and the ground is again impervious.

#### 4. CONCLUSIONS AND RECOMMENDATIONS

The analytical results presented herein are promising and suggest that further work be directed toward empirical validation of the proposed techniques. Specifically, based on this study we conclude the following

1. Structural-acoustic tests, with stationary sources, provide a viable technique for measuring transfer functions relating sonic boom overpressures in the vicinity of a structure to its response, either in terms of displacements, velocities or accelerations.

2. Such transfer functions may be used to perform damage assessments in terms of measurable quantities in the absence of dedicated flyovers.

3. Structural-acoustic reciprocal tests, whereby structures are mechanically driven and the radiated pressure monitored by an array of microphones, may be used to supplement direct testing and increase the practicality and efficiency of performing the required measurements.

4. The structural-acoustic transfer function concept, direct or reciprocal, is modular and allows for easy synthesis and updating with related work, for example improved codes for predicting ground level sonic boom spectra.

5. General purpose structural-acoustic finite element/boundary element (FE/BE) computer codes, introduce a powerful relatively new tool for predicting the response of structures to sonic boom overpressures potentially accounting for both geometric and structural complexities. (For structures modelled as linear systems the predictions inherently satisfy the appropriate reciprocal relationships.)

6. Damage predictions using reciprocal measurements may be quantitative with levels of confidence comparable to those with current techniques. Predictions may also be qualitative, providing a ranking of vulnerability among different structures and environments or among potential damage mechanisms within a given structure. In either case such measurements, perhaps supplemented by FE/BE analyses, provide a valuable input to those responsible for site planning and development in environments vulnerable to supersonic operations.

Consequently, we recommend that the proposed techniques be pursued further. Specifically we recommend the following:

1. Both direct and reciprocal structural-acoustic testing techniques for measuring transfer functions relating sonic boom overpressures to structural response be empirically validated by comparison with equivalent data taken at a series of dedicated sites/structures with actual flyovers.

2. Flyover data should also be used to validate predictions from corresponding detailed FE/BE structural-acoustic numerical models.

3. Upon successful completion of items 1 and 2, procedures be codified to obtain required structural-acoustic transfer functions and integrate them into an overall damage assessment package that includes current estimates of sonic boom overpressure spectra from flight characteristics and propagation factors, and correlations of structural response functions to damage for conventional and unconventional structures.

## REFERENCES

1. R.L. Hershey and T.H. Higgins, Statistical Model of Sonic Boom Structural Damage, Final Report FAA-RD-76-87, 1976.
2. Louis C. Sutherland, Ron Brown and Dawn Goerner, Evaluation of Potential Damage to Unconventional Structures by Sonic Booms, Wyle Research Report WR 89-14, prepared for Dept. of the Air Force, (OL-AC HSD/YA-NSBIT), January 1990.
3. F.V. Hunt, Stress and Strain Limits on the Attainable Velocity in Mechanical Vibration, J. Acoust. Soc. Am. 32, 9, September 1960. Also,
4. Stephen H. Crandall, Relation Between Strain and Velocity in Resonant Vibration, J. Acoust. Soc. Am. 34, 12, December 1962.
5. Carl E. Hanson, et al, HMMH, Inc. Report No. 290940.04.1, prepared for National Park Service under NPS-DSC Contract No. CX-2000-0.0025, September 1991.
6. John F. Wiss, Vibrations During Construction Operations, J. Const. Div. AM. Soc. Civil Engin., 239-245, September 1974.
7. Lord Rayleigh, The Theory of Sound, 2nd Ed. Dover, New York, 1945, p. 45-157.
8. Yu. I. Belousov and A.V. Rimskii-Korsakov, The Reciprocity Principle in Acoustics and Its Application to the Calculation of Sound Fields of Bodies, Sov. Phys. Acoust., Vol. 21, 2, 103-109, 1975.
9. L.M. Lyamshev, "Theory of Sound Radiation by Thin Elastic Shells and Plates," Sov. Phys. Acoust. 5, 431, 1959.

10. P.W. Smith, Jr., "Response and Radiation of Structural Modes Excited by Sound," J. Acoust. Soc. Am. 34, 640-647, 1962.
11. G. Chertock, "Transient Flexural Vibrations of Ship-like Structures Exposed to Underwater Explosions," J. Acoust. Soc. Am. 48, 170-180, 1970.
12. H.F. Olson, Elements of Acoustical Engineering, 2nd ed. (Van Nostrand, New York, 1947), pp. 345-348.
13. I.L. Ver, Reciprocity as a Prediction and Diagnostic Tool in Reducing Transmission of Structureborne and Airborne Noise Into an Aircraft Fuselage - Volume 1: Proof of Feasibility, BBN Report 4985 prepared for NASA Langley Research Center, 21 April 1982.
14. T. ten Wolde, "Reciprocity Experiments on the Transmission of Sound in Ships," (Drukkerit Hoogland Enwaltman, N.V., Delft, 1973. Also, "On the Validity and Application of Reciprocity in Acoustical, Mechano-Acoustical and Other Dynamical Systems, Acustica, Vol. 28, 23-32, (1973).
15. M.C. Junger and D. Feit, Sound, Structures, and Their Interaction, 2nd ed. MIT Press, Cambridge, MA 1986.
16. Ibid, Ch. 5.
17. G.C. Everstine and F.M. Henderson, "Coupled Finite Element/Boundary Element Approach For Fluid-Structure Interaction," J. Acoust. Soc. Am. 87, 1938-1947 (1990).
18. H.A. Schenck, "Improved Integral Formulation for Acoustic Radiation Problems," J. Acoust. Soc. Am., Vol. 44, pp. 41-58 (1968).

19. Mark R. Legg and Jerold M. Haber, Seismic Response of Sonic Boom-Coupled Rayleigh Waves, NSBIT Human Systems Division, Air Force Systems Command, Brooks AFB, TX Report HSD-TR-90-025, June 1990.

20. Leonid M. Brekhovskikh, Waves in Layered Media, Academic Press, New York (1960) p. 31.

21. W.M. Ewing, W.S. Jardetsky and F. Press, Elastic Waves in Layered Media, McGraw Hill, New York, (1957) p. 41. (The notation has been changed and the acoustic impedance added, for consistency with the previous analysis.)

22. M.C. Junger and D. Feit, Sound, Structures and Their Interaction, MIT Press, Cambridge, 2nd Ed. (1986) ch. 5.